Finite temperature fermionic condensate in a conical space with a circular boundary and magnetic flux

Aram A. Saharian,[1,*] Eugênio R. Bezerra de Mello,[2,†] and Astghik A. Saharyan[3,‡]

[1]*Department of Physics, Yerevan State University, 1 Alex Manoogian Street, 0025 Yerevan, Armenia*
[2]*Departamento de Física, Universidade Federal da Paraí ba, 58.059-970, Caixa Postal 5.008, João Pessoa, PB, Brazil*
[3]*Laboratoire Interdisciplinaire Carnot de Bourgogne, CNRS UMR 6303, Université Bourgogne Franche-Comté, BP 47870, F-21078 Dijon, France*

(Received 2 September 2019; published 18 November 2019)

We investigate the edge effects on the finite temperature fermionic condensate (FC) for a massive fermionic field in a $(2+1)$-dimensional conical spacetime with a magnetic flux located at the cone apex. The field obeys the bag boundary condition on a circle concentric with the apex. The analysis is presented for both the fields realizing two irreducible representations of the Clifford algebra and for the general case of the chemical potential. In both the regions outside and inside the circular boundary, the FC is decomposed into the boundary-free and boundary-induced contributions. They are even functions under the simultaneous change of the signs for the magnetic flux and the chemical potential. The dependence of the FC on the magnetic flux becomes weaker with decreasing planar angle deficit. For points near the boundary, the effects of finite temperature, of planar angle deficit, and of magnetic flux are weak. For a fixed distance from the boundary and at high temperatures the FC is dominated by the Minkowskian part. The FC in parity and time-reversal symmetric $(2+1)$-dimensional fermionic models is discussed and applications are given to graphitic cones.

DOI: 10.1103/PhysRevD.100.105014

I. INTRODUCTION

The investigation of field theoretical models in spatial dimensions D other than 3 is motivated by several reasons. Many high-energy theories unifying physical interactions are formulated in higher-dimensional spaces, $D > 3$, with compactified extra dimensions. Examples of these kinds of models include Kaluza-Klein theories, supergravity, and various types of string/M theories. In recent years the models with $D < 3$ has attracted a great deal of attention. Because of lower dimension they are easier to handle and are treated as simplified models in particle physics. The models in dimensions $D < 3$ appear as high temperature limits of $D = 3$ field theories and also as effective theories describing the long-wavelength dynamics of excitations in condensed matter systems [1–4]. The examples for these kinds of systems include graphene made structures (such as a graphene sheet, carbon nanotubes, nanoloops, and nanoribbons), topological insulators, Weyl semimetals, and high-temperature superconductors. In the continuous limit, the long-wavelength properties of these systems are well described by the Dirac equation for fermionic fields living in $(2+1)$-dimensional spacetime with the Fermi velocity instead of the velocity of light [5–7]. This offers the remarkable possibility to probe field theoretical effects in condensed matter systems. Interesting features in $(2+1)$-dimensional models include fractionalization of quantum numbers, the possibility of the excitations with fractional statistics, flavor symmetry breaking, and parity violation. In the corresponding gauge theories, the presence of topologically nontrivial gauge invariant terms in the action provides an interesting possibility to give masses for gauge bosons [8,9]. The infrared cutoff induced by the topological mass term provides a way to solve the infrared problem without changing the ultraviolet behavior.

In the present paper we investigate the combined effects of nontrivial topology, induced by a conical defect, and of a circular boundary on the finite temperature fermionic condensate (FC) for a massive fermionic field in $(2+1)$-dimensional spacetime. In order to have an exactly solvable problem in the region inside the boundary, a simplified model for the defect will be used with a pointlike core. The FC is among the most important local characteristics of a given state for a fermionic field. It carries also important

*saharian@ysu.am
†emello@fisica.ufpb.br
‡astghik.saharyan@gmail.com

information about the global properties of the background spacetime. The FC plays a central role in the models of dynamical breaking of chiral symmetry (for chiral symmetry breaking in models with nontrivial topology and in curved specitimes see [10]). The vacuum FC, the vacuum expectation values of the charge and current densities, and of the energy-momentum tensor for a fermionic field in the geometry under consideration have been investigated in [11–13]. The finite temperature effects for the FC and for the charge and current densities in a boundary-free $(2+1)$-dimensional conical space were discussed in [14] (for the corresponding effects in $(3+1)$-dimensional spacetime with a cosmic string see [15]).

The $(3+1)$-dimensional analog of the setup we are going to consider here is the geometry of an infinite straight cosmic string with coaxial cylindrical boundary. The combined effects of the topology and boundary on the properties of the quantum vacuum in that geometry have been considered for electromagnetic [16–18], scalar [18,19], and fermionic [20] fields. The Casimir forces for massless scalar fields with Dirichlet and Neumann boundary conditions in the geometry of a conical piston are investigated in [21]. The scalar and electromagnetic Casimir densities in the presence of boundaries perpendicular to the string axis are discussed in [22–26]. Another type of boundary condition on quantum fields arises for a cosmic string compactified along its axis. The influence of the compactification on the properties of the quantum vacuum were investigated in [27].

The organization of the paper is as follows. In the next section we describe the bulk and boundary geometries and the field and present complete sets of fermionic modes outside and inside a circular boundary. By using those modes, in Sec. III, the FC in the exterior region is evaluated. It is presented in the form where the boundary-free and boundary-induced contributions are explicitly separated. The properties of the latter are investigated in various asymptotic regions of the parameters. A similar investigation for the interior region is presented in Sec. IV. We also discuss the FC for the second type of boundary condition differing from the previous one by the sign of the term with the normal to the boundary. The parity and time-reversal invariant fermionic models in $(2+1)$ dimensions can be constructed by combining two spinor fields realizing two inequivalent representations of the Clifford algebra. The FC in this class of models and corresponding applications to graphitic cones are discussed in Sec. V. The main results of the paper are summarized in Sec. VI. In the Appendix A we describe the evaluation of the FC for a field with zero chemical potential and show that, although the evaluation procedure is different, the final result can be obtained from the corresponding expression for the nonzero chemical potential taking the zero chemical potential limit. In Appendix B we consider the zero temperature limit and show that both the representations for the FC give the same result.

II. PROBLEM SETUP AND THE FERMIONIC MODES

In this section we describe the bulk and boundary geometries for the problem under consideration and present A complete set of fermionic modes outside and inside a circular boundary. The metric tensor for the background geometry is given by the $(2+1)$-dimensional line element

$$ds^2 = g_{\mu\nu}dx^\mu dx^\nu = dt^2 - dr^2 - r^2 d\phi^2, \tag{2.1}$$

with the spatial coordinates defined in the ranges $r \geq 0$ and $0 \leq \phi \leq \phi_0$. For $\phi_0 = 2\pi$ this corresponds to the standard $(2+1)$-dimensional Minkwoski spacetime. In the case $\phi_0 < 2\pi$ one has a planar angle deficit $2\pi - \phi_0$ and the spatial geometry presents a cone with the apex at $r = 0$. In what follows, in addition to ϕ_0 we will also use the parameter $q = 2\pi/\phi_0$, assuming that $q \geq 1$. We will consider the case of a two-component spinor field $\psi(x)$ realizing the irreducible representation of the Clifford algebra. Also we assume the presence of an external electromagnetic field with the vector potential A_μ. The field operator obeys the Dirac equation

$$(i\gamma^\mu D_\mu - sm)\psi(x) = 0, \quad D_\mu = \partial_\mu + \Gamma_\mu + ieA_\mu, \tag{2.2}$$

where Γ_μ is the spin connection and e the charge of the field quanta. Here, $s = +1$ and $s = -1$ correspond to two inequivalent irreducible representations of the Clifford algebra in $(2+1)$ dimensions (see the discussion in Sec. V below). With these representations, the mass term violates the parity and time-reversal invariances [8]. In the coordinates corresponding to (2.1), the gamma matrices can be taken in the representation

$$\gamma^0 = \begin{pmatrix} 1 & 0 \\ 0 & -1 \end{pmatrix}, \quad \gamma^l = \frac{i^{2-l}}{r^{l-1}} \begin{pmatrix} 0 & e^{-iq\phi} \\ (-1)^{l-1} e^{iq\phi} & 0 \end{pmatrix}, \tag{2.3}$$

with $l = 1, 2$.

We consider the vector potential of the form $A_\mu = (0, 0, A)$, where $A_2 = A$ represents the angular component in the coordinates system defined by (t, r, ϕ). For the physical component of the vector potential one has $A_\phi = -A/r$. This corresponds to an infinitely thin magnetic flux $\Phi = -\phi_0 A$ located at $r = 0$. As it will be seen below, in the expressions for the FC the parameter A enters in the form of the combination

$$\alpha = eA/q = -e\Phi/(2\pi). \tag{2.4}$$

We decompose it as

$$\alpha = \alpha_0 + n_0, \quad |\alpha_0| < 1/2, \tag{2.5}$$

with n_0 being an integer. As we will see the FC depends only on the fractional part α_0 only.

Now we assume the presence of the circular boundary at $r = a$ on which the field obeys the MIT bag boundary condition

$$(1 + i n_\mu \gamma^\mu)\psi(x) = 0, \quad r = a, \tag{2.6}$$

with n_μ being the inward pointing unit vector normal to the boundary. One has $n_\mu = \delta^1_\mu$ and $n_\mu = -\delta^1_\mu$ in the regions $r \le a$ and $r \ge a$, respectively. The main objective of this paper is to investigate the influence of the boundary on the FC assuming that the field is in thermal equilibrium at temperature T. The FC is defined as

$$\langle \bar\psi\psi\rangle = \mathrm{tr}[\hat\rho\,\bar\psi\,\psi], \tag{2.7}$$

where $\bar\psi = \psi^\dagger\gamma^0$ is the Dirac adjoint and the angular brackets denote the ensemble average with the density matrix

$$\hat\rho = \frac{1}{Z} e^{-\beta(\hat H - \mu'\hat Q)}, \qquad \beta = \frac{1}{T}. \tag{2.8}$$

Here $\hat H$ is the Hamilton operator, $\hat Q$ is a conserved charge with the related chemical potential μ', and $Z = \mathrm{tr}[e^{-\beta(\hat H - \mu'\hat Q)}]$.

Let $\{\psi^{(+)}_\sigma(x), \psi^{(-)}_\sigma(x)\}$ be a complete orthonormal set of the positive- and negative-energy solutions of the field equation (2.2), specified by a set of quantum numbers σ. Expanding the field operator $\psi(x)$ in terms of $\psi^{(\pm)}_\sigma(x)$, the FC is decomposed as

$$\langle \bar\psi\psi\rangle = \langle \bar\psi\psi\rangle_{\mathrm{vac}} + \langle \bar\psi\psi\rangle_{T+} + \langle \bar\psi\psi\rangle_{T-}. \tag{2.9}$$

Here,

$$\langle \bar\psi\psi\rangle_{\mathrm{vac}} = \sum_\sigma \bar\psi^{(-)}_\sigma(x)\psi^{(-)}_\sigma(x) \tag{2.10}$$

is the FC in the vacuum state and $\langle \bar\psi\psi\rangle_{T\pm}$ are the contributions from particles (upper sign) and antiparticles (lower signs). They are given by

$$\langle \bar\psi\psi\rangle_{T\pm} = \pm\sum_\sigma \frac{\bar\psi^{(\pm)}_\sigma(x)\psi^{(\pm)}_\sigma(x)}{e^{\beta(E_\sigma \mp \mu)} + 1}, \tag{2.11}$$

where $\mu = e\mu'$ and $\pm E_\sigma$ are the energies corresponding to the modes $\psi^{(\pm)}_\sigma(x)$. In (2.10) and (2.11), $\sum_\sigma$ includes the summation over the discrete quantum numbers and the integration over the continuous ones. The modes are normalized in accordance with the standard normalization condition

$$\int d^2x r \psi^{(\pm)\dagger}_\sigma(x)\psi^{(\pm)}_{\sigma'}(x) = \delta_{\sigma\sigma'}, \tag{2.12}$$

where the radial integration goes over the region under consideration. The part in the FC corresponding to the vacuum expectation value, $\langle \bar\psi\psi\rangle_{\mathrm{vac}}$, has been investigated in [11] and here we will be mainly concerned with the finite temperature parts $\langle \bar\psi\psi\rangle_{T\pm}$. In order to evaluate these parts we need to specify the mode functions $\psi^{(\pm)}_\sigma(x)$.

First let us consider the exterior region, $r \ge a$. The corresponding mode functions are specified by the quantum numbers (γ, j), with $0 \le \gamma < \infty$, $j = \pm 1/2, \pm 3/2, \ldots$, and have the form

$$\psi^{(\pm)}_\sigma(x) = c^{(\pm)}_{\mathrm{e}} e^{iqj\phi \mp iEt} \begin{pmatrix} g^{(\pm)}_{\beta_j,\beta_j}(\gamma a, \gamma r)e^{-iq\phi/2} \\ \epsilon_j \frac{\gamma e^{iq\phi/2}}{\pm E + sm} g^{(\pm)}_{\beta_j,\beta_j+\epsilon_j}(\gamma a, \gamma r) \end{pmatrix}, \tag{2.13}$$

where $E = E_\sigma = \sqrt{\gamma^2 + m^2}$, $\epsilon_j = 1$ for $j > -\alpha$ and $\epsilon_j = -1$ for $j < -\alpha$,

$$\beta_j = q|j + \alpha| - \epsilon_j/2. \tag{2.14}$$

The function $g^{(\pm)}_{\beta_j,\nu}(\gamma a, \gamma r)$, with $\nu = \beta_j$ and $\nu = \beta_j + \epsilon_j$, is expressed in terms of the Bessel and Neumann functions as

$$g^{(\pm)}_{\beta_j,\nu}(\gamma a, \gamma r) = \bar Y^{(\pm)}_{\beta_j}(\gamma a) J_\nu(\gamma r) - \bar J^{(\pm)}_{\beta_j}(\gamma a) Y_\nu(\gamma r). \tag{2.15}$$

Here the notation with the bar is defined as

$$\begin{aligned} \bar F^{(\pm)}_{\beta_j}(z) &= zF'_{\beta_j}(z) - \left(\pm\sqrt{z^2 + m_a^2} + sm_a + \epsilon_j\beta_j\right)F_{\beta_j}(z) \\ &= -\epsilon_j z F_{\beta_j+\epsilon_j}(z) - \left(\pm\sqrt{z^2 + m_a^2} + sm_a\right)F_{\beta_j}(z), \end{aligned} \tag{2.16}$$

and $m_a = ma$. The relative coefficient of the linear combination of the Bessel and Neumann functions in (2.15) is determined by the boundary condition (2.6). The normalization coefficient $c^{(\pm)}_{\mathrm{e}}$ is obtained from the condition (2.12) with the radial integration over $[a, \infty)$ and with $\delta_{\sigma\sigma'} = \delta(\gamma - \gamma')\delta_{jj'}$. It is given by

$$|c^{(\pm)}_{\mathrm{e}}|^2 = \frac{\gamma}{2\phi_0 E} \frac{E \pm sm}{\bar J^{(\pm)2}_{\beta_j}(\gamma a) + \bar Y^{(\pm)2}_{\beta_j}(\gamma a)}. \tag{2.17}$$

In the interior region, $r \le a$, the mode functions are given as

$$\psi_{\sigma}^{(\pm)}(x) = c_{\mathrm{i}}^{(\pm)} e^{iqj\phi \mp iEt} \begin{pmatrix} J_{\beta_j}(\gamma r) e^{-iq\phi/2} \\ \epsilon_j \frac{\gamma e^{iq\phi/2}}{\pm E + sm} J_{\beta_j + \epsilon_j}(\gamma r) \end{pmatrix}. \tag{2.18}$$

From the boundary condition (2.6) it follows that the eigenvalues of γ are solutions of the equation

$$\tilde{J}_{\beta_j}^{(\pm)}(\gamma a) = 0, \tag{2.19}$$

where the notation with tilde for the cylinder functions is defined as

$$\begin{aligned} \tilde{F}_{\beta_j}^{(\pm)}(z) &= zF'_{\beta_j}(z) + \left(\pm\sqrt{z^2 + m_a^2} + sm_a - \epsilon_j \beta_j\right) F_{\beta_j}(z) \\ &= -\epsilon_j z F_{\beta_j + \epsilon_j}(z) + \left(\pm\sqrt{z^2 + m_a^2} + sm_a\right) F_{\beta_j}(z). \end{aligned} \tag{2.20}$$

We denote the positive roots of Eq. (2.19) by $\gamma a = \gamma_{j,l}^{(\pm)}$, $l = 1, 2, \ldots$. It can be seen that the modes for the positive energy solution with $j > -\alpha$ coincide with the modes for negative energy solution with $j < -\alpha$ if we replace $\alpha \to -\alpha$ (particles replaced by antiparticles).

The normalization constant $c_{\mathrm{i}}^{(\pm)}$ is determined from (2.12) with the radial integration over $[0, a]$ and $\delta_{\sigma\sigma'} = \delta_{ll'}\delta_{jj'}$:

$$c_{\mathrm{i}}^{(\pm)2} = \frac{\gamma}{2\phi_0 a} \frac{E \pm sm}{E} T_{\beta_j}(\gamma a), \tag{2.21}$$

where we have defined

$$T_{\beta_j}^{(\pm)}(z) = \frac{z J_{\beta_j}^{-2}(z)}{z^2 + (sm_a - \epsilon_j \beta_j)(sm_a \pm aE) \mp \frac{z^2}{2aE}}, \quad z = \gamma a. \tag{2.22}$$

with $aE = \sqrt{z^2 + m_a^2}$ and $z = \gamma_{j,l}^{(\pm)}$.

We have determined complete sets of fermionic mode functions outside and inside the circular boundary with the boundary condition (2.6) on it. At this point two comments should be made. The radial functions of the modes are solutions of the Bessel equation. In the exterior region these functions are uniquely determined by the boundary condition on the circle $r = a$. Inside the circular boundary and for $2|\alpha_0| \le 1 - 1/q$ the fermionic modes are uniquely determined by the normalizability condition and, as the solution of the Bessel equation, the function $J_{\beta_j}(\gamma r)$ must be taken. In the case $2|\alpha_0| > 1 - 1/q$ and for the mode with $j = -\mathrm{sgn}(\alpha_0)/2$ both the solutions with the functions $J_{\beta_j}(\gamma r)$ and $Y_{\beta_j}(\gamma r)$ are normalizable. The general solution is a linear combination of these functions. One of the coefficients is determined from the normalization conditions of the modes. In order to determine the second coefficient, a boundary condition on the cone apex must be specified. Here the situation is similar to that for the region around an Aharonov-Bohm gauge field. For the latter problem it is well known that the theory of von Neumann deficiency indices leads to a one-parameter family of allowed boundary conditions [28] (see also [29] for a discussion related to graphene with a topological defect). The boundary condition for our choice of the modes (2.18) in the case $j = -\mathrm{sgn}(\alpha_0)/2$ corresponds to the situation when the bag boundary condition is imposed on the circle $r = \varepsilon$ with small $\varepsilon > 0$ and then the limit $\varepsilon \to 0$ is taken.

The second comment is related to the periodicity condition with respect to the rotation around the apex. The mode functions (2.13) and (2.18) are periodic with respect to that rotation: $\psi_{\sigma}^{(\pm)}(t, r, \phi + \phi_0) = \psi_{\sigma}^{(\pm)}(t, r, \phi)$. We can consider a more general quasiperiodicity condition

$$\psi_{\sigma}^{(\pm)}(t, r, \phi + \phi_0) = e^{2\pi i\chi} \psi_{\sigma}^{(\pm)}(t, r, \phi), \tag{2.23}$$

with a constant phase $2\pi\chi$. The corresponding mode functions are simply obtained from (2.13) and (2.18) by the replacement $j \to j + \chi$. The physical results will depend on A and χ in the form of the combination $\tilde{\alpha} = \alpha + \chi = eA/q + \chi$. Though the separate terms α and χ are gauge dependent, the combination $\tilde{\alpha}$ is gauge invariant. The results for a field obeying the quasiperiodicity condition with the phase $2\pi\chi$ are obtained from those given below by the replacement $\alpha \to \tilde{\alpha}$.

III. FC IN THE EXTERIOR REGION

Having specified the mode functions, we start our investigation for the FC in the exterior region. In that region, the FC in the vacuum state is decomposed as [11]

$$\langle \bar{\psi}\psi \rangle_{\mathrm{vac}} = \langle \bar{\psi}\psi \rangle_{\mathrm{vac}}^{(0)} + \langle \bar{\psi}\psi \rangle_{\mathrm{vac}}^{(b)}, \tag{3.1}$$

where the FC for the vacuum state in the boundary-free geometry is given by the expression

$$\begin{aligned} \langle \bar{\psi}\psi \rangle_{\mathrm{vac}}^{(0)} = -\frac{sm}{2\pi r} \Bigg\{ &\sum_{l=1}^{[q/2]} (-1)^l \frac{\cot(\pi l/q)}{e^{2mr\sin(\pi l/q)}} \cos(2\pi l \alpha_0) \\ &- \frac{q}{\pi} \int_0^\infty dy \frac{e^{-2mr\cosh y}}{\cosh y} \frac{f_1(q, \alpha_0, y)}{\cosh(2qy) - \cos(q\pi)} \Bigg\}, \end{aligned} \tag{3.2}$$

with $[q/2]$ being the integer part of $q/2$ and

$$\begin{aligned} f_1(q, \alpha_0, y) = -\sinh y \sum_{\delta = \pm 1} &\cos(q\pi(1/2 - \delta\alpha_0)) \\ &\times \sinh((1 + 2\delta\alpha_0)qy). \end{aligned} \tag{3.3}$$

For the boundary-induced contribution in the vacuum state one has

$$\langle\bar{\psi}\psi\rangle_{\rm vac}^{(b)} = -\frac{1}{\pi\phi_0}\sum_j\int_m^\infty dx\,x\left\{{\rm Im}\left[\frac{\bar{I}_{\beta_j}(xa)}{\bar{K}_{\beta_j}(xa)}\right]\right.\times[K^2_{\beta_j}(xr)+K^2_{\beta_j+\epsilon_j}(xr)]\left.+sm{\rm Re}\left[\frac{\bar{I}_{\beta_j}(xa)}{\bar{K}_{\beta_j}(xa)}\right]\frac{K^2_{\beta_j+\epsilon_j}(xr)-K^2_{\beta_j}(xr)}{\sqrt{x^2-m^2}}\right\}, \quad (3.4)$$

where for the modified Bessel functions we use the notation

$$\bar{F}_{\beta_j}(u) = uF'_{\beta_j}(u) - \left(i\sqrt{u^2-m_a^2}+sm_a+\epsilon_j\beta_j\right)F_{\beta_j}(u). \quad (3.5)$$

Note that for $1 \le q < 2$ the first term in figure braces of (3.2) is absent. Here we are interested in the finite temperature contributions.

Taking into account (2.11) and (2.13), after some intermediate steps we get

$$\langle\bar{\psi}\psi\rangle_{T\pm} = \pm\frac{1}{2\phi_0}\sum_j\int_0^\infty d\gamma\frac{\gamma/E}{e^{\beta(E\mp\mu)}+1}\times\frac{(E\pm sm)g^{(\pm)2}_{\beta_j,\beta_j}(\gamma a,\gamma r)-(E\mp sm)g^{(\pm)2}_{\beta_j,\beta_j+\epsilon_j}(\gamma a,\gamma r)}{\bar{J}^{(\pm)2}_{\beta_j}(\gamma a)+\bar{Y}^{(\pm)2}_{\beta_j}(\gamma a)}. \quad (3.6)$$

In order to find an explicit expression for the boundary-induced part, we subtract from (3.6) the corresponding boundary-free term $\langle\bar{\psi}\psi\rangle^{(0)}_{T\pm}$. The expression for the latter is obtained from (3.6) by the replacements $g^{(\pm)2}_{\beta_j,\nu}(x,y)/[\bar{J}^{(\pm)2}_{\beta_j}(x)+\bar{Y}^{(\pm)2}_{\beta_j}(x)] \to J^2_\nu(y)$ with $\nu=\beta_j$ and $\nu=\beta_j+\epsilon_j$ (see [14]). For the evaluation of the boundary-induced part, we use the identity

$$\frac{g^{(\pm)2}_{\beta_j,\nu}(x,y)}{\bar{J}^{(\pm)2}_{\beta_j}(x)+\bar{Y}^{(\pm)2}_{\beta_j}(x)} - J^2_\nu(y) = -\frac{1}{2}\sum_{l=1,2}\frac{\bar{J}^{(\pm)}_{\beta_j}(x)}{\bar{H}^{(l,\pm)}_{\beta_j}(x)}H^{(l)2}_\nu(y), \quad (3.7)$$

valid for both $\nu=\beta_j,\beta_j+\epsilon_j$, and with $H^{(l)}_\nu(x)$ being the Hankel functions. In this way, for the boundary-induced parts

$$\langle\bar{\psi}\psi\rangle^{(b)}_{T\pm} = \langle\bar{\psi}\psi\rangle_{T\pm} - \langle\bar{\psi}\psi\rangle^{(0)}_{T\pm} \quad (3.8)$$

we get

$$\langle\bar{\psi}\psi\rangle^{(b)}_{T\lambda} = -\lambda\frac{1}{4\phi_0}\sum_j\sum_{l=1,2}\int_0^\infty d\gamma\frac{\gamma}{E}\frac{\bar{J}^{(\lambda)}_{\beta_j}(\gamma a)}{\bar{H}^{(l,\lambda)}_{\beta_j}(\gamma a)}\times\frac{(E+\lambda sm)H^{(l)2}_{\beta_j}(\gamma r)-(E-\lambda sm)H^{(l)2}_{\beta_j+\epsilon_j}(\gamma r)}{e^{\beta(E-\lambda\mu)}+1}, \quad (3.9)$$

with $\lambda=\pm$. For the further transformation of (3.9) we will assume that $\mu\neq0$. The case $\mu=0$ will be considered in Appendix A.

The integrand in (3.9) has simple poles for

$$E = E^{(\lambda)}_n \equiv \lambda\mu + i\pi(2n+1)T, \quad (3.10)$$

with $n=0,\pm1,\pm2,\ldots$. One has $n=0,1,2,\ldots$ for the poles in the upper half-plane and $n=\ldots,-2,-1$ in the lower half-plane. For the values of $\gamma=\gamma^{(\lambda)}_n$ corresponding to the poles (3.10) we get

$$\gamma^{(\lambda)2}_n = [\lambda\mu + i\pi(2n+1)T]^2 - m^2, \quad (3.11)$$

where, again, $n=0,1,2,\ldots$ ($n=\ldots,-2,-1$) for the poles in the upper (lower) half-plane. Note that for the poles in the upper and lower half-planes one has the relations

$$E^{(\lambda)}_n = E^{(\lambda)*}_{-n-1}, \quad \gamma^{(\lambda)}_n = \gamma^{(\lambda)*}_{-n-1}, \quad n=\ldots,-2,-1, \quad (3.12)$$

where the star stands for the complex conjugate.

For the transformation of (3.9) we rotate the integration contour in the complex plane γ by the angle $\pi/2$ for the term with $l=1$ and by the angle $-\pi/2$ for the term with $l=2$. For $\lambda\mu<0$ the thermal factor $1/[e^{\beta(E-\lambda\mu)}+1]$ has no poles in the right half-plane and the integral is transformed to the integrals over the imaginary axis. In the case $\lambda\mu>0$, in addition to the latter integrals the residue terms from the poles (3.11) should be added. In the integral over the positive imaginary semiaxis we introduce the modified Bessel functions $I_\nu(z)$ and $K_\nu(z)$ by using the relations

$$\bar{J}^{(\lambda)}_{\beta_j}(e^{\pi i/2}z) = e^{i\pi\beta_j/2}\bar{I}^{(\lambda)}_{\beta_j}(z),$$
$$\bar{H}^{(1,\lambda)}_{\beta_j}(e^{\pi i/2}z) = \frac{2}{\pi i}e^{-i\pi\beta_j/2}\bar{K}^{(\lambda)}_{\beta_j}(z), \quad (3.13)$$

where for the modified Bessel functions we use the notation

$$\bar{F}^{(\lambda)}_{\beta_j}(z) = zF'_{\beta_j}(z) - \left(\lambda\sqrt{(e^{\pi i/2}z)^2+m_a^2}+sm_a+\epsilon_j\beta_j\right)F_{\beta_j}(z), \quad (3.14)$$

with $F=I,K$. For the functions in the integral over the negative imaginary semiaxis one has $\bar{J}^{(\lambda)}_{\beta_j}(e^{-\pi i/2}z) = e^{i\pi\beta_j/2}\bar{I}^{(\lambda)*}_{\beta_j}(z)$ and $\bar{H}^{(2,\lambda)}_{\beta_j}(e^{-\pi i/2}z) = -\frac{2}{\pi i}e^{i\pi\beta_j/2}\bar{K}^{(\lambda)*}_{\beta_j}(z)$. Note that for $z\ge0$ the square root is understood as

$$\sqrt{(e^{\pm\pi i/2}z)^2+m_a^2}=\begin{cases}\sqrt{m_a^2-z^2}, & z<m_a,\\ e^{\pm\pi i/2}\sqrt{z^2-m_a^2}, & z>m_a.\end{cases} \tag{3.15}$$

From here it follows that $\bar{F}^{(\lambda)*}_{\beta_j}(z)=\bar{F}^{(\lambda)}_{\beta_j}(z)$ for $z<m_a$. By using this relation we can see that the integrals over the intervals $(0, im_a)$ and $(0, -im_a)$ cancel each other. For $\lambda\mu>0$, the contributions to $\langle\bar{\psi}\psi\rangle^{(T)}_{b,\lambda}$ from the residue terms at the poles in the upper and lower half-planes are combined as

$$-\lambda\frac{\pi}{\phi_0}\theta(\lambda\mu)T\sum_j\sum_{n=0}^{\infty}\mathrm{Im}\left\{\frac{\bar{J}^{(\lambda)}_{\beta_j}(\gamma_n^{(\lambda)}a)}{\bar{H}^{(1,\lambda)}_{\beta_j}(\gamma_n^{(\lambda)}a)}\times[(E_n^{(\lambda)}+\lambda sm)H^{(1)2}_{\beta_j}(\gamma_n^{(\lambda)}r)-(E_n^{(\lambda)}-\lambda sm)H^{(1)2}_{\beta_j+\epsilon_j}(\gamma_n^{(\lambda)}r)]\right\}, \tag{3.16}$$

where $\theta(x)$ is the Heaviside step function and for the poles in the lower half-plane we have used the relations (3.12). We find it convenient to introduce in (3.16) a new quantity $u_n^{(\lambda)}$ in accordance with $\gamma_n^{(\lambda)}=iu_n^{(\lambda)}$, $\mathrm{Re}u_n^{(\lambda)}>0$,

$$u_n^{(\lambda)}=\{[\pi(2n+1)T-i\lambda\mu]^2+m^2\}^{1/2}. \tag{3.17}$$

Note that $u_n^{(-)}=u_n^{(+)*}$.

After the transformations described above, the boundary-induced contribution in the thermal part of the FC is presented as

$$\langle\bar{\psi}\psi\rangle^{(b)}_{T\lambda}=\lambda\frac{1}{\pi\phi_0}\sum_j\int_m^{\infty}dx\,x\mathrm{Im}\left\{\frac{\bar{I}^{(\lambda)}_{\beta_j}(xa)}{\bar{K}^{(\lambda)}_{\beta_j}(xa)}\frac{1}{e^{\beta(i\sqrt{x^2-m^2}-\lambda\mu)}+1}\left[\left(1-\frac{i\lambda sm}{\sqrt{x^2-m^2}}\right)K^2_{\beta_j}(xr)+\left(1+\frac{i\lambda sm}{\sqrt{x^2-m^2}}\right)K^2_{\beta_j+\epsilon_j}(xr)\right]\right\}$$
$$-\lambda\frac{2}{\phi_0}\theta(\lambda\mu)T\sum_j\sum_{n=0}^{\infty}\mathrm{Im}\left\{\frac{\bar{I}^{(\lambda)}_{\beta_j}(u_n^{(\lambda)}a)}{\bar{K}^{(\lambda)}_{\beta_j}(u_n^{(\lambda)}a)}[(\pi(2n+1)T-i\lambda(\mu+sm))K^2_{\beta_j}(u_n^{(\lambda)}r)+(\pi(2n+1)T-i\lambda(\mu-sm))K^2_{\beta_j+\epsilon_j}(u_n^{(\lambda)}r)]\right\}. \tag{3.18}$$

By taking into account the relations $\bar{I}^{(-)}_{\beta_j}(xa)=\bar{I}^{(+)*}_{\beta_j}(xa)$, $\bar{K}^{(-)}_{\beta_j}(xa)=\bar{K}^{(+)*}_{\beta_j}(xa)$, we can see that for $\lambda=-$ the expressions under the sign of the summation over n in (3.18) differs from that for $\lambda=+$ by the sign. As a consequence, the expression (3.18) is transformed to

$$\langle\bar{\psi}\psi\rangle^{(b)}_{T\lambda}=\frac{1}{\pi\phi_0}\sum_j\int_m^{\infty}dx\,x\mathrm{Im}\left\{\frac{\bar{I}_{\beta_j}(xa)}{\bar{K}_{\beta_j}(xa)}\frac{1}{e^{\lambda\beta(i\sqrt{x^2-m^2}-\mu)}+1}\left[\left(1-\frac{ism}{\sqrt{x^2-m^2}}\right)K^2_{\beta_j}(xr)+\left(1+\frac{ism}{\sqrt{x^2-m^2}}\right)K^2_{\beta_j+\epsilon_j}(xr)\right]\right\}$$
$$-\frac{2}{\phi_0}\theta(\lambda\mu)T\sum_j\sum_{n=0}^{\infty}\mathrm{Im}\left\{\frac{\bar{I}_{\beta_j}(u_na)}{\bar{K}_{\beta_j}(u_na)}[(\pi(2n+1)T-i(\mu+sm))K^2_{\beta_j}(u_nr)+(\pi(2n+1)T-i(\mu-sm))K^2_{\beta_j+\epsilon_j}(u_nr)]\right\}. \tag{3.19}$$

Here

$$u_n=\{[\pi(2n+1)T-i\mu]^2+m^2\}^{1/2}, \tag{3.20}$$

and for the modified Bessel functions we use the notation $\bar{F}_{\beta_j}(z)=\bar{F}^{(+)}_{\beta_j}(z)$, defined by (3.5) with $F=I, K$. The expressions (3.19) with $\lambda=+$ and $\lambda=-$ present the contributions to the boundary-induced FC coming from particles and antiparticles.

Combining the contribution from the separate terms for $\lambda=+$ and $\lambda=-$, we can see that in evaluating the boundary-induced part $\langle\bar{\psi}\psi\rangle^{(b)}_T=\sum_{\lambda=\pm}\langle\bar{\psi}\psi\rangle^{(b}_{T\lambda}$ the sum of the first terms on the right-hand side of (3.19) is equal to $-\langle\bar{\psi}\psi\rangle^{(b)}_{\mathrm{vac}}$ with $\langle\bar{\psi}\psi\rangle^{(b)}_{\mathrm{vac}}$ from (3.4). Hence, the boundary-induced contribution at temperature T, given by

$$\langle\bar{\psi}\psi\rangle^{(b)}=\langle\bar{\psi}\psi\rangle^{(b)}_{\mathrm{vac}}+\langle\bar{\psi}\psi\rangle^{(b)}_T, \tag{3.21}$$

is presented in the form

$$\langle\bar{\psi}\psi\rangle^{(b)} = -\frac{2T}{\phi_0}\sum_j\sum_{n=0}^{\infty}\mathrm{Im}\left\{\frac{\bar{I}_{\beta_j}(u_n a)}{\bar{K}_{\beta_j}(u_n a)}\right. \times[(\pi(2n+1)T-i(\mu+sm))K^2_{\beta_j}(u_n r) \left. +(\pi(2n+1)T-i(\mu-sm))K^2_{\beta_j+\epsilon_j}(u_n r)]\right\}. \tag{3.22}$$

The ratio under the imaginary part in this expression can be written in the form

$$\frac{\bar{I}_{\beta_j}(z)}{\bar{K}_{\beta_j}(z)} = \frac{W^{(-)}_{\beta_j,\beta_j+\epsilon_j}(z) + [i\pi(2n+1)T+\mu]a/z}{z[K^2_{\beta_j+\epsilon_j}(z)+K^2_{\beta_j}(z)] + 2sm_a K_{\beta_j}(z)K_{\beta_j+\epsilon_j}(z)}, \tag{3.23}$$

with the notation (the notation with the $+$ sign will appear in the expression for the FC in the interior region)

$$W^{(\pm)}_{\beta_j,\beta_j+\epsilon_j}(z) = z[I_{\beta_j}(z)K_{\beta_j}(z) - I_{\beta_j+\epsilon_j}(z)K_{\beta_j+\epsilon_j}(z)] \pm sm_a[I_{\beta_j+\epsilon_j}(z)K_{\beta_j}(z) - I_{\beta_j}(z)K_{\beta_j+\epsilon_j}(z)], \tag{3.24}$$

and with $z = u_n a$.

For the total FC one has

$$\langle\bar{\psi}\psi\rangle = \langle\bar{\psi}\psi\rangle^{(0)} + \langle\bar{\psi}\psi\rangle^{(b)}, \tag{3.25}$$

where $\langle\bar{\psi}\psi\rangle^{(0)}$ is the FC at temperature T in the absence of the boundary [14]. The notation with bar in (3.22) can also be presented in the form

$$\bar{F}_{\beta_j}(z) = \delta_F z F_{\beta_j+\epsilon_j}(z) - (i\sqrt{z^2-m_a^2} + sm_a)F_{\beta_j}(z), \tag{3.26}$$

where $\delta_I = -\delta_K = 1$. Under the replacements $\alpha\to-\alpha$, $j\to-j$ one has $\beta_j \rightleftarrows \beta_j+\epsilon_j$. By using this and the representation (3.26), it can be seen that under the same replacements we get

$$\frac{\bar{I}_{\beta_j}(u_n a)}{\bar{K}_{\beta_j}(u_n a)} \to -\left[\frac{\bar{I}_{\beta_j}(u_n^* a)}{\bar{K}_{\beta_j}(u_n^* a)}\right]^*. \tag{3.27}$$

Now, by taking into account the relation $u_n^*(\mu) = u_n(-\mu)$, one can show that $\langle\bar{\psi}\psi\rangle^{(b)}$ is an even function under the simultaneous replacements $\alpha\to-\alpha$, $\mu\to-\mu$.

In [14], the boundary-free contribution is presented in the form

$$\langle\bar{\psi}\psi\rangle^{(0)} = \langle\bar{\psi}\psi\rangle^{(0)}_{\mathrm{M}} + \langle\bar{\psi}\psi\rangle^{(0)}_{\mathrm{t}}, \tag{3.28}$$

where

$$\langle\bar{\psi}\psi\rangle^{(0)}_{\mathrm{M}} = \frac{smT}{2\pi}[\ln(1+e^{-(m-\mu)/T}) + \ln(1+e^{-(m+\mu)/T})], \tag{3.29}$$

is the FC in $(2+1)$-dimensional Minkowski spacetime (the magnetic flux and the planar angle deficit are absent, $q=1$, $\alpha=0$) and $\langle\bar{\psi}\psi\rangle^{(0)}_{\mathrm{t}}$ is the topological part induced by the conical geometry and by the magnetic flux. The latter is given by the expression [14]

$$\langle\bar{\psi}\psi\rangle^{(0)}_{\mathrm{t}} = -\frac{2mT}{\pi}\sum_{n=-\infty}^{\infty}\left\{s\sum_{l=1}^{[q/2]}(-1)^l c_l\cos(2\pi l\alpha_0)K_0(2rs_l u_n) - \frac{sq}{\pi}\int_0^\infty dy\frac{f_1(q,\alpha_0,y)K_0(2ru_n\cosh y)}{\cosh(2qy)-\cos(q\pi)}\right. \left. +\frac{\mu+i\pi(2n+1)T}{m}\left[\sum_{l=1}^{[q/2]}(-1)^l s_l\sin(2\pi l\alpha_0)K_0(2rs_l u_n) - \frac{q}{\pi}\int_0^\infty dy\frac{f_2(q,\alpha_0,y)K_0(2ru_n\cosh y)}{\cosh(2qy)-\cos(q\pi)}\right]\right\}, \tag{3.30}$$

where $c_l = \cos(\pi l/q)$, $s_l = \sin(\pi l/q)$, and

$$f_2(q,\alpha_0,y) = \cosh y\sum_{\delta=\pm1}\delta\cos(q\pi(1/2-\delta\alpha_0))\cosh((1+2\delta\alpha_0)qy). \tag{3.31}$$

The representation (3.30) is well adapted for the investigation of high-temperature asymptotic. An alternative representation, convenient in the low-temperature limit, is provided in Ref. [14].

In the case of zero chemical potential, $\mu=0$, the poles of the integrand in (3.9) are located on the imaginary axis and the procedure for the transformation is different from what we have described above. This case is considered in Appendix A, where it has been shown that the final result is obtained from (3.22) in the limit $\mu\to0$. The corresponding expression can also be presented in the form

$$\langle\bar{\psi}\psi\rangle^{(b)} = -\frac{2T}{\phi_0}\sum_j\sum_{n=0}^{\infty}\left\{\pi(2n+1)T\mathrm{Im}\left[\frac{\bar{I}_{\beta_j}(u_{0n}a)}{\bar{K}_{\beta_j}(u_{0n}a)}\right][K^2_{\beta_j}(u_{0n}r) + K^2_{\beta_j+\epsilon_j}(u_{0n}r)]\right. \left. - sm\mathrm{Re}\left[\frac{\bar{I}_{\beta_j}(u_{0n}a)}{\bar{K}_{\beta_j}(u_{0n}a)}\right][K^2_{\beta_j}(u_{0n}r) - K^2_{\beta_j+\epsilon_j}(u_{0n}r)]\right\}, \tag{3.32}$$

where u_{0n} is defined by

$$u_{0n} = \sqrt{[\pi(2n+1)T]^2 + m^2}. \tag{3.33}$$

The boundary-induced FC (3.32) is an even function of α. The ratio under the imaginary and real parts is presented in the form (3.23), where now $z = u_{0n}r$ is real and the imaginary and real parts are easily separated. The expression (3.32) is further simplified for a massless field:

$$\langle\bar{\psi}\psi\rangle^{(b)} = -\frac{2T}{\phi_0 a}\sum_j \sum_{n=0}^{\infty} \frac{K^2_{\beta_j}(ur) + K^2_{\beta_j+\epsilon_j}(ur)}{K^2_{\beta_j}(ua) + K^2_{\beta_j+\epsilon_j}(ua)}\bigg|_{u=\pi(2n+1)T}. \tag{3.34}$$

Of course, in this case the FC does not depend on the parameter s. The corresponding boundary-free part vanishes, $\langle\bar{\psi}\psi\rangle^{(0)} = 0$ (see [14]), and the total FC $\langle\bar{\psi}\psi\rangle = \langle\bar{\psi}\psi\rangle^{(b)}$ is always negative. It is a monotonically increasing function of the radial coordinate r.

Now we move to the investigation of the boundary-induced FC in asymptotic regions for the values of the parameters. For general values of the chemical potential and the mass, at large distances from the boundary, in (3.22) we use the asymptotic expression of the Macdonald function for large arguments. To leading order this gives

$$\langle\bar{\psi}\psi\rangle^{(b)} \approx -\frac{qT}{r}\sum_j \sum_{n=0}^{\infty} \mathrm{Im}\left\{\frac{\bar{I}_{\beta_j}(u_n a)}{\bar{K}_{\beta_j}(u_n a)}\frac{e^{-2u_n r}}{u_n} \times [\pi(2n+1)T - i\mu]\right\}. \tag{3.35}$$

For $T \gtrsim m, |\mu|$ the dominant contribution comes from the term $n = 0$ and the boundary-induced contribution is suppressed by the factor e^{-2ru_0}. For $q < 2$, a similar suppression takes place for the topological part $\langle\bar{\psi}\psi\rangle^{(0)}_{\mathrm{t}}$ in the boundary-free geometry. For $q > 2$, the suppression of the latter at large distances is weaker, by the factor $e^{-2ru_0 \sin(\pi/q)}$. The Minkowskian part (3.29) does not depend on the radial coordinate and for a massive field it dominates at large distances. For a massless field with zero chemical potential and for $Tr \gg 1$ one has

$$\langle\bar{\psi}\psi\rangle^{(b)} \approx -\frac{2e^{-2\pi Tr}}{\phi_0 ar}\sum_j \frac{1}{K^2_{\beta_j}(\pi Ta) + K^2_{\beta_j+\epsilon_j}(\pi Ta)}. \tag{3.36}$$

Hence, the boundary-induced FC is exponentially suppressed at large distances. Note that at large distances the boundary-induced contribution in the vacuum FC behaves like $\langle\bar{\psi}\psi\rangle^{(b)}_{\mathrm{vac}} \propto e^{-2mr}/r^2$, $mr \gg 1$, for a massive field and as $\langle\bar{\psi}\psi\rangle^{(b)}_{\mathrm{vac}} \propto 1/r^{q(1-2|\alpha_0|)+2}$ in the case of a massless field.

In the high temperature limit, $T \gg m, |\mu|, 1/(r-a)$, again, the contribution of the $n = 0$ term dominates in (3.22) and, similar to (3.35), we can see that the boundary-induced FC for a given r is suppressed by the factor $e^{-2\pi Tr}$. For the boundary-free topological part we have similar behavior, $\langle\bar{\psi}\psi\rangle^{(0)}_{\mathrm{t}} \propto e^{-2\pi Tr}$ for $q < 2$. In the case $q > 2$ one has $\langle\bar{\psi}\psi\rangle^{(0)}_{\mathrm{t}} \propto e^{-2\pi Tr\sin(\pi/q)}$ and the decay is slower. As a consequence, at high temperatures and for points not too close to the boundary, the total FC is dominated by the Minkowskian part that behaves like $\langle\bar{\psi}\psi\rangle^{(0)}_{\mathrm{M}} \approx smT\ln 2/(2\pi)$.

The boundary-induced FC (3.22) diverges on the boundary. This kind of surface divergence in the vacuum expectation values (VEVs) of local physical observables are well known in quantum field theory with boundaries. They are related to the idealized boundary conditions on fields acting in the same way for all the modes of the field. For points near the boundary, assuming that $T(r-a) \ll 1$, the dominant contribution to the series over n in (3.22) comes from large n and, to the leading order, we can replace the corresponding summation by the integration. In Appendix B, it is shown that, with this replacement, the corresponding expectation value is obtained for the vacuum state. Hence, we conclude that for points near the boundary and for temperatures $T \ll 1/(r-a)$ the finite temperature effects on the FC are small and the leading term coincides with the vacuum FC. Near the boundary the latter is dominated by the boundary-induced part and behaves as $\langle\bar{\psi}\psi\rangle_{\mathrm{vac}} \approx \langle\bar{\psi}\psi\rangle^{(b)}_{\mathrm{vac}} \approx -1/[8\pi(r-a)^2]$. Note that this leading term does not depend on the planar angle deficit or the magnetic flux.

It is also of interest to consider the behavior of the boundary-induced FC for small values of the radius a and for fixed r, assuming that $Ta, ma \ll 1$. By using the asymptotic expressions for the modified Bessel functions for small values of the argument, from (3.22) one can see that $\langle\bar{\psi}\psi\rangle^{(b)} \propto a^{q(1-2|\alpha_0|)}$ and for $|\alpha_0| < 1/2$ the boundary-induced contribution tends to zero in the limit $a \to 0$. In the special case $|\alpha_0| = 1/2$ the part $\langle\bar{\psi}\psi\rangle^{(b)}$ tends to a finite limiting value. The case $|\alpha_0| = 1/2$ is also special for the boundary-free geometry. For example, the VEVs of the charge and current densities, as functions of the parameter α from (2.4), are discontinuous at the points corresponding to half-odd-integer values of α (see, e.g., Ref. [12]). In accordance with (2.5), this corresponds to the case $|\alpha_0| = 1/2$. A similar feature for the persistent current in carbon nanotube based rings has been observed in Ref. [30]. Note that the VEVs of the charge and current densities in the region $r > a$ vanish for $|\alpha_0| = 1/2$.

The numerical examples for the dependence of the FC on the parameters of the problem will be given for a simple case of a massless field with a zero chemical potential (for the effects of the nonzero mass see Fig. 5). In the boundary-free geometry the FC vanishes and the nonzero FC is

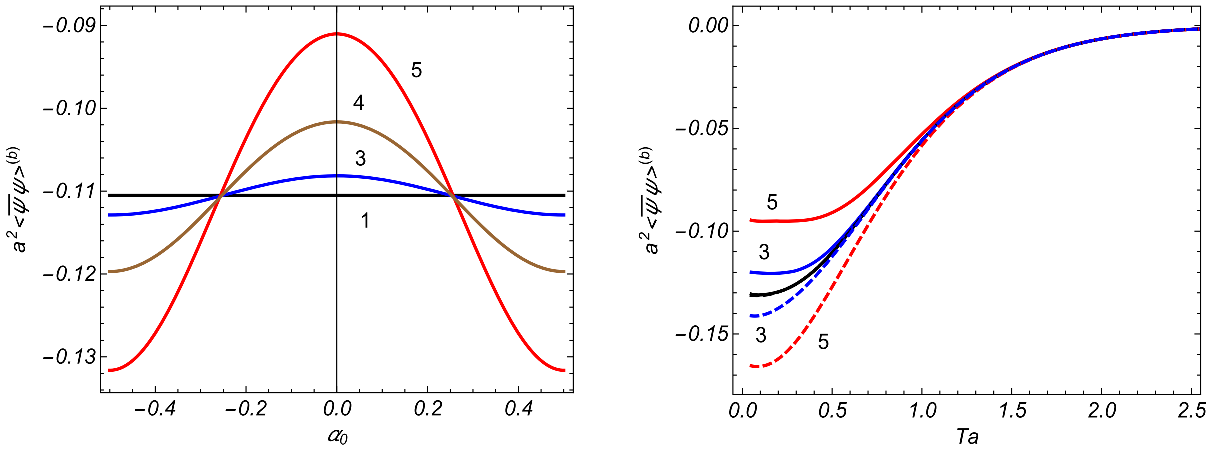

FIG. 1. FC in the exterior region for a massless field with a zero chemical potential versus the parameter α_0 (left) and the temperature (right). The graphs are plotted for $r/a = 1.5$ and the numbers near the curves correspond to the values of q. For the left panel we have taken $Ta = 0.5$. The full/dashed curves in the right panel correspond to $\alpha_0 = 0/\alpha_0 = 0.4$.

induced by the boundary. The left panel in Fig. 1 displays the FC in the exterior region versus the parameter α_0 for fixed values of $r/a = 1.5$, $Ta = 0.5$. The numbers near the curves correspond to the values of the parameter q. As seen, for small values of the planar angle deficit, the dependence of the FC on the magnetic flux is weak. In the right panel of Fig. 1 we have plotted the FC versus the temperature (in units of $1/a$) for $r/a = 1.5$. The numbers near the curves are the values of the parameter q and the full (dashed) curves correspond to $\alpha_0 = 0$ ($\alpha_0 = 0.4$). For $q = 1$ (the curve between the full and dashed curves for $q = 3$) the dependence of the FC on α_0 is weak and for that case the full and dashed curves are almost the same. As seen from the graphs, the dependence on the magnetic flux becomes weaker with decreasing planar angle deficit (decreasing q). In accordance with the asymptotic analysis given above, the suppression of the FC at high temperatures is seen in the right panel.

The dependence of the FC on the radial coordinate is shown in the left panel of Fig. 2 for fixed temperature corresponding to $Ta = 0.5$. The numbers near the curves present the values of the parameter q. The full and dashed curves correspond to $\alpha_0 = 0$ and $\alpha_0 = 0.4$, respectively. Again, for $q = 1$ (the curves between the full and dashed curves for $q = 3$) the curves for $\alpha_0 = 0$ and $\alpha_0 = 0.4$ are almost the same. As it has been shown above by the asymptotic analysis, for large values of Tr the FC is suppressed by the factor $e^{-2\pi Tr}$. The dependence of the FC in the exterior region on the planar angle deficit is displayed in the right panel of Fig. 2 for $r/a = 1.5$,

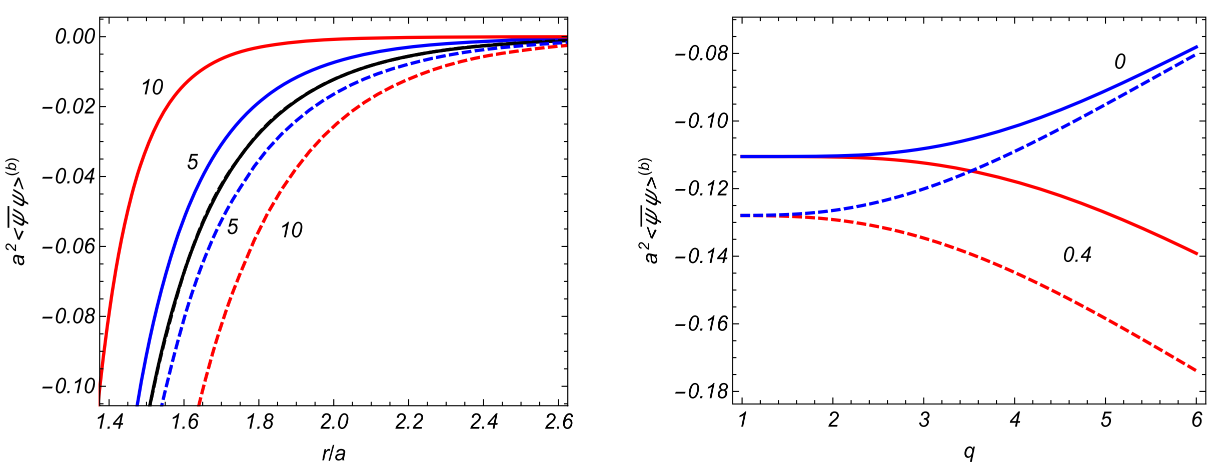

FIG. 2. FC in the exterior region for a massless field with a zero chemical potential as a function of the radial coordinate (left) and of the parameter q (right). For the left panel $Ta = 0.5$ and the full/dashed curves correspond to $\alpha_0 = 0/\alpha_0 = 0.4$. The numbers near the curves are the values of q. The right panel is plotted for $r/a = 1.5$, $Ta = 0.5$ (full curves), $Ta = 0.25$ (dashed curves) and the numbers near the curves are the corresponding values of α_0.

$Ta = 0.5$ (full curves) and $Ta = 0.25$ (dashed curves). The figures near the curves correspond to the values of the parameter α_0. As seen from the right panel, the behavior of the boundary-induced FC as a function of q is essentially different for $\alpha_0 = 0$ and $\alpha_0 = 0.4$.

Note that the boundary $r = a$ separates the exterior region from the region where the magnetic flux is located. As a consequence of that, the results presented in this section are valid for an arbitrary distribution of the magnetic flux in the region $r < a$.

IV. FC INSIDE A CIRCULAR BOUNDARY

In this section we consider the region $r \leq a$. The corresponding FC in the vacuum state is presented as (3.1), where the boundary-induced contribution is given by [11]

$$\langle \bar{\psi}\psi \rangle^{(b)}_{\mathrm{vac}} = -\frac{1}{\pi\phi_0}\sum_j \int_m^\infty dx\, x \left\{ \mathrm{Im}\left[\frac{\tilde{K}_{\beta_j}(xa)}{\tilde{I}_{\beta_j}(xa)}\right][I^2_{\beta_j}(xr) + I^2_{\beta_j+\epsilon_j}(zr)] + sm\mathrm{Re}\left[\frac{\tilde{K}_{\beta_j}(xa)}{\tilde{I}_{\beta_j}(xa)}\right]\frac{I^2_{\beta_j+\epsilon_j}(zr) - I^2_{\beta_j}(xr)}{\sqrt{x^2-m^2}} \right\}, \quad (4.1)$$

with the notation for the modified Bessel functions

$$\tilde{F}_{\beta_j}(u) = uF'_{\beta_j}(u) + \left(i\sqrt{u^2 - m_a^2} + sm_a - \epsilon_j\beta_j\right)F_{\beta_j}(u), \quad (4.2)$$

where $F = I, K$.

Substituting the fermionic modes (2.18) in the mode-sum formula (2.11), for the contributions of the positive and negative energy modes to the thermal part in the FC one gets

$$\langle \bar{\psi}\psi \rangle_{T\lambda} = \lambda \frac{1}{2\phi_0 a^2}\sum_j \sum_{l=1}^\infty \frac{T_{\beta_j}(\gamma^{(\lambda)}_{j,l})g(\gamma^{(\lambda)}_{j,l})}{e^{\beta(E^{(\lambda)}_{j,l}-\lambda\mu)}+1}, \quad (4.3)$$

where $\lambda = +,-$, $E^{(\lambda)}_{j,l} = \sqrt{\gamma^{(\lambda)2}_{j,l}/a^2 + m^2}$, $z = \gamma^{(\lambda)}_{j,l}$ are the positive zeros of the function $\tilde{J}^{(\lambda)}_{\beta_j}(z)$ defined in accordance with (2.20) and we have introduced the notation

$$g(z) = z\left[\left(1 + \frac{\lambda s m_a}{\sqrt{z^2 + m_a^2}}\right)J^2_{\beta_j}(zr/a) - \left(1 - \frac{\lambda s m_a}{\sqrt{z^2 + m_a^2}}\right)J^2_{\beta_j+\epsilon_j}(zr/a)\right]. \quad (4.4)$$

The roots $\gamma^{(\lambda)}_{j,l}$ are given implicitly and the representation (4.3) is not convenient for the evaluation of the FC. The summation formula for series of the type $\sum_{l=1}^\infty T_{\beta_j}(\gamma^{(\lambda)}_{j,l})f(\gamma^{(\lambda)}_{j,l})$ has been derived in [31] by using the generalized Abel-Plana formula from [32,33] assuming that the function $f(z)$ is analytic in the right half-plane of the complex variable z. In the problem at hand

$$f(z) = \frac{g(z)}{e^{\beta(\sqrt{z^2/a^2+m^2}-\lambda\mu)}+1}, \quad (4.5)$$

and for $\lambda\mu > 0$ this function has simple poles $z = \gamma^{(\lambda)}_n$, $n = 0, \pm 1, \pm 2, \ldots$, in the right half-plane (the case $\mu = 0$ when the poles are located on the imaginary axis will be discussed in Appendix A).

The procedure described in [31] can be generalized keeping the terms in the generalized Abel-Plana formula coming from the poles in the right half-plane. For the functions $f(x)$ real for real values of x, this leads to the following summation formula:

$$\sum_{l=1}^\infty T_{\beta_j}(\gamma^{(\lambda)}_{j,l})f(\gamma^{(\lambda)}_{j,l}) = \int_0^\infty dx\, f(x) + \frac{\pi}{2}\operatorname*{Res}_{z=0}\frac{\tilde{Y}^{(\lambda)}_{\beta_j}(z)}{\tilde{J}^{(\lambda)}_{\beta_j}(z)}f(z) - 4\sum_{n=0}^\infty \mathrm{Re}\left[e^{-i\pi\beta_j}\frac{\tilde{K}^{(\lambda)}_{\beta_j}(u^{(\lambda)}_n)}{\tilde{I}^{(\lambda)}_{\beta_j}(u^{(\lambda)}_n)}\operatorname*{Res}_{z=iu^{(\lambda)}_n}f(z)\right] - \frac{2}{\pi}\int_0^\infty dx\,\mathrm{Re}\left[e^{-\beta_j\pi i}f(xe^{\pi i/2})\frac{\tilde{K}^{(\lambda)}_{\beta_j}(x)}{\tilde{I}^{(\lambda)}_{\beta_j}(x)}\right], \quad (4.6)$$

where $u^{(\lambda)}_n = -i\gamma^{(\lambda)}_n$ and for the modified Bessel functions we have defined the notation

$$\tilde{F}^{(\lambda)}_{\beta_j}(z) = zF'_{\beta_j}(z) + \left(\lambda\sqrt{(e^{\pi i/2}z)^2 + m_a^2} + sm_a - \epsilon_j\beta_j\right)F_{\beta_j}(z), \quad (4.7)$$

with $F = I, K$. The second term on the right-hand side of (4.6) comes from the poles of the function $f(z)$ in the right half-plane. For an analytic function $f(z)$ the formula (4.6) is reduced to the one in [31].

In the problem at hand the function $f(z)$ is given by (4.5). For this function the integrand in the last term of (4.6) vanishes for $x < m_a$. The residue term at $z = 0$ vanishes as well. The part in $\langle \bar{\psi}\psi \rangle_{T\lambda}$ coming from the first integral on the right-hand side of (4.6) presents the corresponding quantity in the boundary-free geometry, denoted here as $\langle \bar{\psi}\psi \rangle^{(0)}_{T\lambda}$. As a result, $\langle \bar{\psi}\psi \rangle_{T\lambda}$ is presented as (3.8), where for the boundary-induced contribution (3.8) one gets

$$\langle\bar{\psi}\psi\rangle_{T\lambda}^{(b)} = \lambda\frac{1}{\pi\phi_0}\sum_j\int_m^\infty dx\,\mathrm{Im}\left\{\frac{\tilde{K}_{\beta_j}^{(\lambda)}(xa)}{\tilde{I}_{\beta_j}^{(\lambda)}(xa)}\frac{x}{e^{\beta(i\sqrt{x^2-m^2}-\lambda\mu)}+1}\left[\left(1-\frac{\lambda ism}{\sqrt{x^2-m^2}}\right)I_{\beta_j}^2(xr)+\left(1+\frac{\lambda ism}{\sqrt{x^2-m^2}}\right)I_{\beta_j+\epsilon_j}^2(zr)\right]\right\}$$
$$-\lambda\frac{2}{\phi_0}\theta(\lambda\mu)T\sum_j\sum_{n=0}^\infty\mathrm{Im}\left\{\frac{\tilde{K}_{\beta_j}^{(\lambda)}(u_n^{(\lambda)}a)}{\tilde{I}_{\beta_j}^{(\lambda)}(u_n^{(\lambda)}a)}[(\pi(2n+1)T-i\lambda(\mu+sm))I_{\beta_j}^2(u_n^{(\lambda)}r)\right.$$
$$\left.+(\pi(2n+1)T-i\lambda(\mu-sm))I_{\beta_j+\epsilon_j}^2(u_n^{(\lambda)}r)]\right\}. \tag{4.8}$$

The further transformation is similar to that for (3.18) with the representation

$$\langle\bar{\psi}\psi\rangle_{T\lambda}^{(b)} = \frac{1}{\pi\phi_0}\sum_j\int_m^\infty dx\,\mathrm{Im}\left\{\frac{\tilde{K}_{\beta_j}(xa)}{\tilde{I}_{\beta_j}(xa)}\frac{x}{e^{\lambda\beta(i\sqrt{x^2-m^2}-\mu)}+1}\left[\left(1-\frac{ism}{\sqrt{x^2-m^2}}\right)I_{\beta_j}^2(xr)+\left(1+\frac{ism}{\sqrt{x^2-m^2}}\right)I_{\beta_j+\epsilon_j}^2(zr)\right]\right\}$$
$$-\frac{2}{\phi_0}\theta(\lambda\mu)T\sum_j\sum_{n=0}^\infty\mathrm{Im}\left\{\frac{\tilde{K}_{\beta_j}(u_na)}{\tilde{I}_{\beta_j}(u_na)}[(\pi(2n+1)T-i(\mu+sm))I_{\beta_j}^2(u_nr)+(\pi(2n+1)T-i(\mu-sm))I_{\beta_j+\epsilon_j}^2(u_nr)]\right\}, \tag{4.9}$$

where the notation with tilde is defined in accordance with (4.2).

Summing the contributions from $\lambda = +$ and $\lambda = -$, we can see that the sum of the first terms on the right-hand side of (4.9) gives $-\langle\bar{\psi}\psi\rangle_{\mathrm{vac}}^{(b)}$. As a consequence, for the boundary-induced contribution (3.21) one finds

$$\langle\bar{\psi}\psi\rangle^{(b)} = -\frac{2T}{\phi_0}\sum_j\sum_{n=0}^\infty\mathrm{Im}\left\{\frac{\tilde{K}_{\beta_j}(u_na)}{\tilde{I}_{\beta_j}(u_na)}[(\pi(2n+1)T-i(\mu+sm))I_{\beta_j}^2(u_nr)+(\pi(2n+1)T-i(\mu-sm))I_{\beta_j+\epsilon_j}^2(u_nr)]\right\}, \tag{4.10}$$

where u_n is defined by (3.20). The total FC is presented as (3.25). An equivalent representation for the notation in (4.10) is given by

$$\tilde{F}_{\beta_j}(u) = \delta_F uF_{\beta_j+\epsilon_j}(u)+\left(i\sqrt{u^2-m_a^2}+sm_a\right)F_{\beta_j}(u). \tag{4.11}$$

Similar to the case of the exterior region, we can see that $\langle\bar{\psi}\psi\rangle^{(b)}$ is an even function under the simultaneous reflections $\alpha\to-\alpha$, $\mu\to-\mu$. In (4.10), the ratio of the modified Bessel functions can be presented in the form

$$\frac{\tilde{K}_{\beta_j}(z)}{\tilde{I}_{\beta_j}(z)} = \frac{W_{\beta_j,\beta_j+\epsilon_j}^{(+)}(z)+[i\pi(2n+1)T+\mu]a/z}{z[I_{\beta_j}^2(z)+I_{\beta_j+\epsilon_j}^2(z)]+2sm_aI_{\beta_j}(z)I_{\beta_j+\epsilon_j}(z)}, \tag{4.12}$$

where $z = u_na$ and $W_{\beta_j,\beta_j+\epsilon_j}^{(+)}(z)$ is defined by (3.24).

The FC in the case $\mu = 0$ is considered in Appendix A. Though the corresponding procedure for the evaluation of (4.10) differs from what we have described above for $\mu\neq 0$, the final result can be obtained from (4.10) taking the limit $\mu\to 0$:

$$\langle\bar{\psi}\psi\rangle^{(b)} = -\frac{2T}{\phi_0}\sum_j\sum_{n=0}^\infty\left\{\pi(2n+1)T\,\mathrm{Im}\left[\frac{\tilde{K}_{\beta_j}(u_{0n}a)}{\tilde{I}_{\beta_j}(u_{0n}a)}\right][I_{\beta_j}^2(u_{0n}r)+I_{\beta_j+\epsilon_j}^2(u_nr)]-sm\,\mathrm{Re}\left[\frac{\tilde{K}_{\beta_j}(u_{0n}a)}{\tilde{I}_{\beta_j}(u_{0n}a)}\right][I_{\beta_j}^2(u_{0n}r)-I_{\beta_j+\epsilon_j}^2(u_{0n}r)]\right\}, \tag{4.13}$$

with u_{0n} from (3.33). Note that now the arguments $u_{0n}a$ are real and the imaginary and real parts in (4.13) are directly obtained from (4.12). For a massless field the expression for the boundary-induced contribution in FC is reduced to

$$\langle\bar{\psi}\psi\rangle^{(b)} = -\frac{2T}{\phi_0 a}\sum_j\sum_{n=0}^\infty\left.\frac{I_{\beta_j}^2(ur)+I_{\beta_j+\epsilon_j}^2(ur)}{I_{\beta_j}^2(ua)+I_{\beta_j+\epsilon_j}^2(ua)}\right|_{u=\pi(2n+1)T}, \tag{4.14}$$

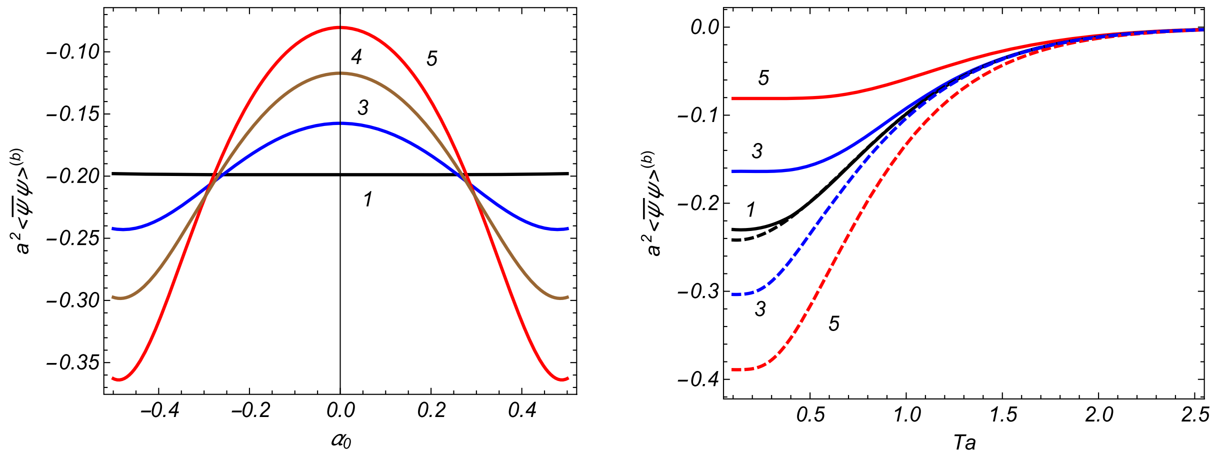

FIG. 3. The same as in Fig. 1 for the interior region with fixed $r/a = 0.5$.

and it is negative. In this special case the boundary-free FC is zero and the total FC is negative as well. For $2|\alpha_0| \leq 1 - 1/q$ the FC given by (4.14) is a monotonically decreasing function of the radial coordinate. That is not the case for $2|\alpha_0| > 1 - 1/q$ when one of the orders of the Bessel modified functions can be negative.

Now we return to a general case of the chemical potential and the mass and consider the behavior of the boundary-induced FC (4.10) near the cone apex corresponding to small values of r. Redefining the summation variable $j + n_0 \to j$, the order β_j of the modified Bessel function is expressed in terms of α_0. It can be seen that in the limit $r \to 0$ the dominant contribution to the FC (4.10) comes from the mode with $j = -\mathrm{sgn}(\alpha_0)/2$. Expanding the Bessel modified function for small values of the argument, to leading order we get

$$\langle\bar{\psi}\psi\rangle^{(b)} \approx -\frac{qT(r/2)^{q-2q|\alpha_0|-1}}{\pi\Gamma^2((q+1)/2 - q|\alpha_0|)} \sum_{n=0}^{\infty} \mathrm{Im}\bigg\{[\pi(2n+1)T - i(\mu - \mathrm{sgn}(\alpha_0)sm)]u_n^{2\beta_j} \frac{\tilde{K}_{\beta_j}(u_n a)}{\tilde{I}_{\beta_j}(u_n a)}\bigg\}, \quad (4.15)$$

where $\beta_j = q(1/2 - |\alpha_0|) + \mathrm{sgn}(\alpha_0)/2$. As seen, the boundary-induced FC vanishes on the cone apex for $2|\alpha_0| < 1 - 1/q$ and diverges for $2|\alpha_0| > 1 - 1/q$. The divergence in the latter case is related to the contribution of the irregular mode at the cone apex. Note that, near the apex, for a massive field the FC in the boundary-free geometry is dominated by the vacuum part and the latter behaves as $1/r$ [14]. Similar to the case of the exterior region, it can be seen that for points near the boundary, under the assumption $T(r - a) \ll 1$, the leading term in the asymptotic expansion over the distance from the boundary coincides with that for the vacuum FC and does not depend on the planar angle deficit and on the magnetic flux. It diverges like $1/(a - r)^2$.

In the expressions for the FC in the exterior and interior regions, for the modified Bessel functions $F_{\beta_j}(u) = I_{\beta_j}(u), K_{\beta_j}(u)$, we have introduced the notations $\bar{F}_{\beta_j}(u)$ and $\tilde{F}_{\beta_j}(u)$. These notations are combined in a single expression

$$F^{(\eta)}_{\beta_j}(u) = uF'_{\beta_j}(u) + \Big[\eta\Big(i\sqrt{u^2 - m_a^2} + sm_a\Big) - \epsilon_j\beta_j\Big]F_{\beta_j}(u) = \delta_F uF_{\beta_j+\epsilon_j}(u) + \eta\Big(i\sqrt{u^2 - m_a^2} + sm_a\Big)F_{\beta_j}(u), \quad (4.16)$$

with $\eta = \pm 1$. For the normal to the boundary one $n_\mu = \eta\delta^1_\mu$, where $\eta = +1$ in the interior region and $\eta = -1$ in the exterior region, and $F^{(+1)}_{\beta_j}(u) = \tilde{F}_{\beta_j}(u)$, $F^{(-1)}_{\beta_j}(u) = \bar{F}_{\beta_j}(u)$.

In Fig. 3, for a massless field with $\mu = 0$, we have presented the dependence of the FC inside a circular boundary on the parameter α_0 and on the temperature for fixed $r/a = 0.5$. For the left panel $Ta = 0.5$ and in the right panel the full and dashed curves correspond to $\alpha_0 = 0$ and $\alpha_0 = 0.4$, respectively. In both the panels, the numbers near the curves correspond to the values of q. Again, we see that for a planar geometry, $q = 1$, the dependence of the FC on the magnetic flux is weak.

In Fig. 4 we display the FC inside a circular boundary as a function of the radial coordinate and of the parameter q. In the left panel the numbers near the curves are the values of the parameter q, the full/dashed curves correspond to $\alpha_0 = 0/\alpha_0 = 0.4$, and the graphs are plotted for $Ta = 0.5$. In the right panel $r/a = 0.5$, $Ta = 0.5$ for full curves and $Ta = 0.25$ for dashed curves. The numbers near the curves correspond to the values of α_0. As it was mentioned above, in the case $2|\alpha_0| > 1 - 1/q$ the FC in the interior region is not a monotonic function of the radial coordinate.

In the numerical examples above we have considered the case of a massless field. It is of interest to consider the effect of the mass on the FC. For a massive field the FC will

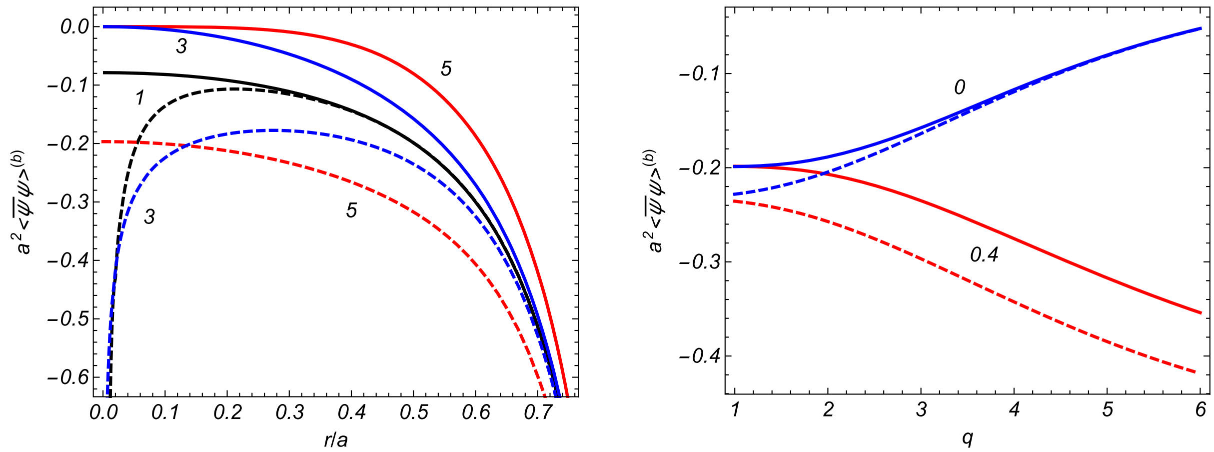

FIG. 4. The same as in Fig. 2 for the interior region. For the right panel we have taken $r/a = 0.5$.

depend on the parameter s. For a field with zero chemical potential, in Fig. 5 we have plotted the dependence of the FC on the mass outside (left panel) and inside (right panel) a circular boundary for a conical space with $q = 2.5$ and for the magnetic flux corresponding to $\alpha_0 = 0.4$. The full and dashed curves correspond to $s = 1$ and $s = -1$, respectively, and the numbers near the curves are the values of Ta. For the left and right panels we have taken $r/a = 1.5$ and $r/a = 0.5$, respectively. As is seen, the influence of the mass on the FC is different for the cases $s = 1$ and $s = -1$. In the first case the absolute value of the FC decreases with increasing mass, whereas in the second case the absolute value of the FC takes its maximum for some intermediate value of the mass parameter. Note that Fig. 5 presents the boundary-induced contribution. For a massive field, there is also a nonzero boundary-free part discussed in [14].

In order to see the importance of the effects of a boundary on the finite temperature FC, let us compare the boundary-induced FC, depicted in Fig. 5 with the corresponding quantity in the boundary-free conical space. First of all, we note that for a massless field the FC in the boundary-free geometry vanishes and the nonzero FC is a purely boundary-induced effect. In this case, the influence of the finite temperature on the FC is seen from Figs. 1 and 3. For a massive field the boundary-free part of the FC is given by Eq. (3.28) with separate contributions from Eqs. (3.29) and (3.30). This part has opposite signs for the cases $s = 1$ and $s = -1$. In Fig. 6 we have displayed the boundary-free FC (full curves) for the case $s = 1$ as a function of the field mass. The left and right panels correspond to $r/a = 1.5$ and $r/a = 0.5$ and in the numerical evaluation we have taken $q = 2.5$ and $\alpha_0 = 0.4$ (the same as in Fig. 5). Similar to Fig. 5, the numbers near the curves correspond to the values of Ta. The dashed curves correspond to the quantity $a^2\langle\bar{\psi}\psi\rangle_{\mathrm{M}}^{(0)}$, where the FC $\langle\bar{\psi}\psi\rangle_{\mathrm{M}}^{(0)}$ in $(2+1)$-dimensional Minkowski spacetime, in the absence of the magnetic flux, is given by (3.29) with $s = 1$. The FC $\langle\bar{\psi}\psi\rangle_{\mathrm{M}}^{(0)}$ does not depend on the radial

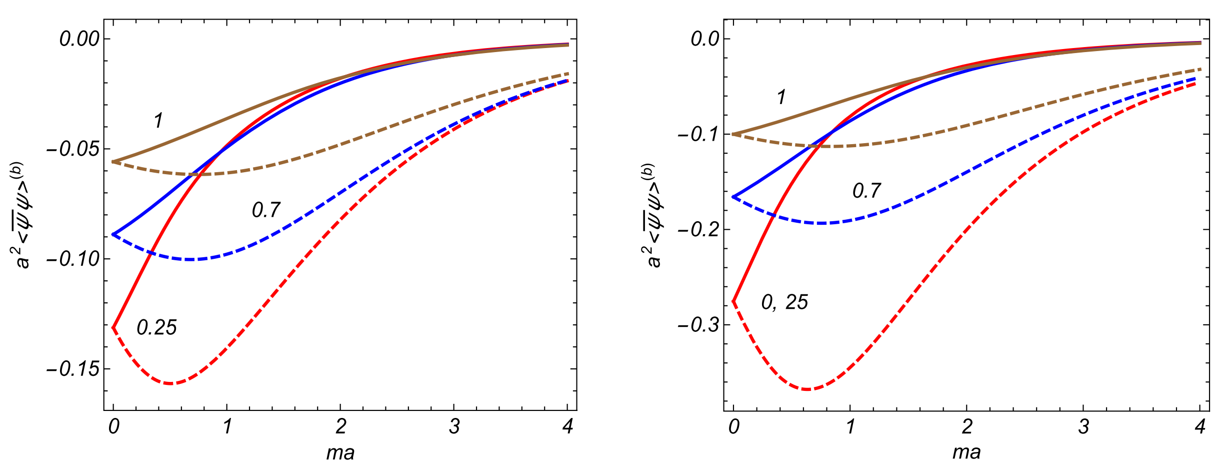

FIG. 5. Boundary-induced FC as a function of the field mass in the case of a zero chemical potential in the exterior (left panel, $r/a = 1.5$) and interior (right panel, $r/a = 0.5$) regions. The full and dashed curves correspond to $s = 1$ and $s = -1$, respectively. The numbers near the curves are the values of Ta and for remaining parameters we have taken $q = 2.5$, $\alpha_0 = 0.4$.

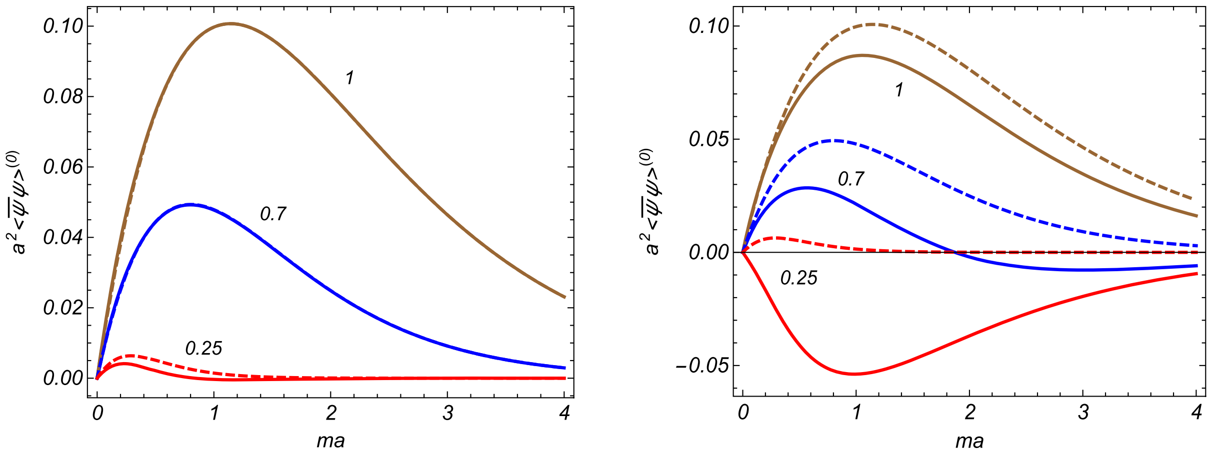

FIG. 6. Boundary-free part in the FC (full curves) versus the field mass in the case of a zero chemical potential and for the field with $s = 1$. The left and right panels are plotted for $r/a = 1.5$ and $r/a = 0.5$, respectively. The dashed curves present the FC in $(2+1)$-dimensional Minkowski spacetime when the magnetic flux is absent. The values of the remaining parameters are the same as those for Fig. 5.

coordinate and the dashed curves on the left and right panels coincide. At large distances from the cone apex the relative contribution of the topological part is small, whereas near the apex it is essential. As seen from the graphs, the topological contribution may change the sign of the FC (the graph for $Ta = 0.25$ on the left panel and the graphs for $Ta = 0.25$, 0.7 on the right panel). Now, comparing the graphs in Figs. 5 and 6, we see that, for the values of the parameters used in the numerical evaluation, the boundary-induced contributions to the finite temperature FC are essential and they may qualitatively change the behavior of the FC.

The geometry inside a circular boundary, discussed in this section, can be considered as a limiting case of a conical ring with a fermionic field localized in the region $b < r < a$ and obeying the MIT bag boundary condition (2.6) on the edges $r = a$, b. Similar to the limiting transition $a \to 0$, discussed in the previous section, we expect that for fixed r and $|\alpha_0| \neq 1/2$, the contribution of the boundary at $r = b$ to the FC will tend to zero in the limit $b \to 0$. Consequently, for Tb, mb, $b/r \ll 1$, the results of this section will approximate the FC in conical rings threaded by a magnetic flux.

We could consider the boundary condition

$$(1 - in_\mu\gamma^\mu)\psi(x) = 0, \tag{4.17}$$

that differs from (2.6) by the sign of the term containing the normal to the boundary. As it has been already noticed in [34], this type of condition is an equally acceptable one for the Dirac equation. The mode functions for the case of boundary condition (4.17) are obtained from the mode functions (2.13) and (2.18) by changing the signs of the terms with $\sqrt{z^2 + m_a^2}$ and sm_a in the definitions of the notations (2.16) and (2.20). The final formulas for the boundary-induced contribution in the FC, $\langle\bar{\psi}\psi\rangle^{(b)}$, are obtained from (3.22) and (4.10) by changing the signs of the terms with $\sqrt{u^2 - m_a^2}$ and sm_a in the notations (3.5) and (4.2). Note that this corresponds to the change $\eta \to -\eta$ in (4.16). Let us denote the boundary-induced FC for given s and μ in the cases of the boundary conditions (2.6) and (4.17) by $\langle\bar{\psi}\psi\rangle_s^{(b,+1)}(\mu)$ and $\langle\bar{\psi}\psi\rangle_s^{(b,-1)}(\mu)$, respectively. The corresponding expressions can be written in combined form

$$\langle\bar{\psi}\psi\rangle_s^{(b,\eta)}(\mu) = -\frac{2T}{\phi_0}\sum_j\sum_{n=0}^{\infty}\mathrm{Im}\left\{\frac{K_{\beta_j}^{(\eta)}(u_n a)}{I_{\beta_j}^{(\eta)}(u_n a)}[(\pi(2n+1)T - i(\mu + sm))I_{\beta_j}^2(u_n r) + (\pi(2n+1)T - i(\mu - sm))I_{\beta_j+\epsilon_j}^2(u_n r)]\right\}, \tag{4.18}$$

in the interior region and

$$\langle\bar{\psi}\psi\rangle_s^{(b,\eta)}(\mu) = -\frac{2T}{\phi_0}\sum_j\sum_{n=0}^{\infty}\mathrm{Im}\left\{\frac{I_{\beta_j}^{(-\eta)}(u_n a)}{K_{\beta_j}^{(-\eta)}(u_n a)}[(\pi(2n+1)T - i(\mu + sm))K_{\beta_j}^2(u_n r) + (\pi(2n+1)T - i(\mu - sm))K_{\beta_j+\epsilon_j}^2(u_n r)]\right\} \tag{4.19}$$

in the exterior region. Here η specifies the boundary condition: $\eta = +1$ for (2.6) and $\eta = -1$ for (4.17). On the basis of these formulas, by taking into account the relations

$$F_{\beta_j}^{(-\eta)}(u_n(-\mu)a)\Big|_{s=\pm1} = [F_{\beta_j}^{(\eta)}(u_n(\mu)a)]^*_{s=\mp1}, \tag{4.20}$$

we see that

$$\langle\bar{\psi}\psi\rangle_s^{(b,-1)}(\mu) = -\langle\bar{\psi}\psi\rangle_{-s}^{(b,+1)}(-\mu). \tag{4.21}$$

This gives the relation between the boundary-induced FCs for the boundary conditions (2.6) and (4.17). In particular, for a massless field with zero chemical potential the FC is given by (3.34) and (4.14) for the boundary condition (2.6) and by the same expressions with the opposite signs for the condition (4.17).

V. FC IN PARITY AND TIME-REVERSAL SYMMETRIC MODELS

As was mentioned above, in $(2+1)$ dimensions one has two inequivalent irreducible representations of the Clifford algebra. These representations can be realized by two sets of 2×2 gamma matrices $\gamma_{(s)}^{\mu} = (\gamma^0, \gamma^1, \gamma_{(s)}^2 = -is\gamma^0\gamma^1/r)$, where γ^0 and γ^1 are given by (2.3) and $s = \pm1$. The representation with $s = +1$ corresponds to γ^2 in (2.3). In separate representations with given s, the mass term in the Lagrangian density $L_s = \bar{\psi}_{(s)}(i\gamma_{(s)}^{\mu}D_\mu - m)\psi_{(s)}$ breaks the parity (P) and time-reversal (T) invariances of the fermionic model. In the absence of magnetic fields, P- and T-invariant models in $(2+1)$ dimensions can be constructed considering a set of two fields $\psi_{(+1)}$ and $\psi_{(-1)}$ with the Lagrangian density $L = \sum_{s=\pm1} L_s$. First let us consider the case when both the fields obey the boundary condition (2.6) on the circle $r = a$:

$$(1 + in_\mu\gamma_{(s)}^{\mu})\psi_{(s)}(x) = 0. \tag{5.1}$$

We can formulate the model in terms of new fields $\psi'_{(s)}$ defined as $\psi'_{(+1)} = \psi_{(+1)}$ and $\psi'_{(-1)} = \gamma^0\gamma^1\psi_{(-1)}$. The Lagrangian density is presented as $L = \sum_{s=\pm1}\bar{\psi}'_{(s)}(i\gamma^\mu D_\mu - sm)\psi'_{(s)}$ with the gamma matrices defined by (2.3) and the Dirac equation for the separate fields is in the form (2.2). The boundary conditions for new fields take the form $(1 + isn_\mu\gamma^\mu)\psi'_{(s)}(x) = 0$. Introducing 4-component spinor $\Psi = (\psi'_{(+1)}, \psi'_{(-1)})^T$ and 4×4 Dirac matrices $\gamma_{(4)}^{\mu} = \sigma_3 \otimes \gamma^\mu$, with $\sigma_3 = \mathrm{diag}(1,-1)$, the Lagrangian density is written as $L = \bar{\Psi}(i\gamma_{(4)}^{\mu}D_\mu - m)\Psi$ with the boundary condition $(1 + in_\mu\gamma_{(4)}^{\mu})\Psi(x) = 0$ on $r = a$. The latter is the bag boundary condition for the 4-component spinor.

For the FC corresponding to the field $\psi_{(s)}$ one has $\langle\bar{\psi}_{(s)}\psi_{(s)}\rangle = s\langle\bar{\psi}'_{(s)}\psi'_{(s)}\rangle$ and for the total FC we get

$$\langle\bar{\Psi}\Psi\rangle = \sum_{s=\pm1}\langle\bar{\psi}_{(s)}\psi_{(s)}\rangle = \sum_{s=\pm1} s\langle\bar{\psi}'_{(s)}\psi'_{(s)}\rangle. \tag{5.2}$$

The expressions for the separate terms in the last sum of (5.2) are obtained from the results of the previous sections. The field $\psi'_{(+1)}$ obeys the same equation and the boundary condition [the condition (2.6)] as the field $\psi(x)$ in Sec. II with $s = +1$ and the boundary-induced contribution to the corresponding FC in the interior and exterior regions is given by (4.18) and (4.19) with $s = 1$ and $\eta = +1$. The field $\psi'_{(-1)}$ obeys the same equation as the field $\psi(x)$ with $s = -1$ and the boundary condition (4.17). The corresponding boundary-induced contribution to the FC is given by (4.18) and (4.19) with $s = -1$ and $\eta = -1$. By taking into account the relation (4.21) we see that

$$\langle\bar{\psi}'_{(-1)}\psi'_{(-1)}\rangle^{(b)}(\mu) = -\langle\bar{\psi}'_{(+1)}\psi'_{(+1)}\rangle^{(b)}(-\mu). \tag{5.3}$$

Hence, the boundary-induced contribution to the total FC is presented in the form

$$\langle\bar{\Psi}\Psi\rangle^{(b)} = \sum_{l=\pm1}\langle\bar{\psi}'_{(+1)}\psi'_{(+1)}\rangle^{(b)}(l\mu), \tag{5.4}$$

where $\langle\bar{\psi}'_{(+1)}\psi'_{(+1)}\rangle^{(b)}(\mu)$ is given by (4.18) and (4.19) with $s = 1$ and $\eta = +1$. By taking into account that $\langle\bar{\psi}'_{(+1)}\psi'_{(+1)}\rangle^{(b)}(\mu)$ is an even function under the transformation $\alpha \to -\alpha$, $\mu \to -\mu$, from (5.4) it follows that the FC $\langle\bar{\Psi}\Psi\rangle^{(b)}$ is an even function of μ and α separately. In the case of the zero chemical potential, $\mu = 0$, we get $\langle\bar{\Psi}\Psi\rangle^{(b)} = 2\langle\bar{\psi}'_{(+1)}\psi'_{(+1)}\rangle^{(b)}$.

We could consider the case when the fields $\psi_{(s)}$ with $s = +1$ and $s = -1$ obey different boundary conditions: $(1 + isn_\mu\gamma_{(s)}^{\mu})\psi_{(s)}(x) = 0$, $r = a$. This type of problem has been discussed in [35] for graphene rings, where the parameter s corresponds to valley degree of freedom (see below). In this case, the transformed fields $\psi'_{(s)}(x)$ obey the same boundary condition $(1 + in_\mu\gamma^\mu)\psi'_{(s)}(x) = 0$. The corresponding condensate $\langle\bar{\psi}'_{(s)}\psi'_{(s)}\rangle^{(b)}$ is given by (4.18) and (4.19) with $\eta = +1$ and the total FC is obtained by using the last relation in (5.2). For a massless field one has $\langle\bar{\psi}'_{(-1)}\psi'_{(-1)}\rangle^{(b)} = \langle\bar{\psi}'_{(+1)}\psi'_{(+1)}\rangle^{(b)}$ and the total FC vanishes $\langle\bar{\Psi}\Psi\rangle^{(b)} = 0$.

Among the condensed matter realizations of the fermionic model we have considered are graphitic cones (carbon nanocones in another terminology). The long-wavelength properties of the corresponding electronic subsystem are well described by a set of two-component spinors $(\psi_{(+1)}, \psi_{(-1)})$, obeying the Dirac equation with the speed of light replaced by the Fermi velocity of electrons (see, e.g., [5]). These spinors correspond to the two different inequivalent points $\mathbf{K}_+$ and $\mathbf{K}_-$ at the corners of the two-dimensional Brillouin zone for the graphene hexagonal lattice. The parameter $s = \pm 1$ in the discussion above corresponds to valley degree of freedom in graphene. The components of the separate spinors $\psi_{(s)}$ give the amplitude of the electron wave function on triangular sublattices A and B of the graphene hexagonal lattice. Graphitic cones are obtained from a planar graphene sheet if one or more sectors with the angle $\pi/3$ are excised and the remainder is joined. The opening angle of the cone is given by $\phi_0 = 2\pi(1 - n_c/6)$, where $n_c = 1, 2, \ldots, 5$ is the number of the removed sectors. The graphitic cones with these values of opening angle have been experimentally observed [36]. The electronic structure of graphitic cones was investigated in [37–43]. Note that the graphitic cones have been observed in both the forms as caps on the ends of the nanotubes and as free-standing structures (see, for instance, [38] and references therein). The geometry outside the circular boundary, which we have considered above, corresponds to the continuum description of graphitic cones with a cut apex. As was discussed in [37], that can be done with acid or with an scanning tunneling microscope. For even values of n_c the periodicity condition for 4-spinor $\Psi = (\psi_{(+1)}, \psi_{(-1)})^T$ under the rotation around the cone apex has the form $\Psi(t, r, \phi + \phi_0) = -\cos(\pi n_c/2)\Psi(t, r, \phi)$ and it does not mix the spinors $\psi_{(+1)}$ and $\psi_{(-1)}$. For $n_c = 2$ this corresponds to the condition we have discussed in the preceding sections and the corresponding FC is obtained by combining the contributions from $s = +1$ and $s = -1$ in the way we have described above. For $n_c = 4$ one has an antiperiodic boundary condition and for the parameter χ in (2.23) we get $\chi = 1/2$. In this case the FC for separate fields $\psi_{(s)}$ are obtained from the formulas given in the preceding sections by the replacement $\alpha \to \alpha + 1/2$. By a gauge transformation this can be interpreted as a shift in the magnetic flux. Note that the Dirac mass m in the formulas given above is expressed in terms of the energy gap Δ in graphene by the relation $m = \Delta/v_F^2$, where $v_F \approx 7.9 \times 10^7$ cm/s is the Fermi velocity of electrons. Depending on the gap generation mechanism, the energy gap varies in the range 1 meV $\lesssim \Delta \lesssim$ 1 eV.

VI. CONCLUSION

We have considered the combined effects of finite temperature and circular boundary on the FC in a $(2 + 1)$-dimensional conical spacetime with an arbitrary value of the planar angle deficit. Two types of boundary conditions were used. The first one corresponds to the MIT bag boundary condition and the second one, given by (4.17), differs by the sign in front of the term containing the normal to the boundary. In two-dimensional spaces there exist two inequivalent representations of the Clifford algebra and we have presented the investigation for both fields realizing those representations. For the evaluation of the FC, the direct summation over a complete set of fermionic modes is employed. In the case of the bag boundary condition those modes outside and inside the circular boundary are given by (2.13) and (2.18). In the region inside the circular boundary the eigenvalues of the radial quantum number γ are roots of Eq. (2.19). They are given implicitly and for the summation of the corresponding series in the mode sum we have generalized the formula from [31] for functions having poles in the right-half plane. That allowed us to present the FC in the form where the explicit knowledge of the eigenvalues for γ is not required.

The FCs in both the exterior and interior regions are decomposed into boundary-free and boundary-induced contributions, as given by (3.25). The boundary-free geometry has been discussed in [14] and we were mainly concerned with the effects induced by the boundary. For a general case of a massive fermionic field with nonzero chemical potential, the boundary-induced contributions in the exterior and interior regions are given by expressions (3.22) and (4.10). They are periodic functions of the magnetic flux with the period equal to the flux quantum and even functions under the simultaneous reflections $\alpha \to -\alpha$, $\mu \to -\mu$. The expressions for the boundary-induced FCs are further simplified for a field with zero chemical potential [see (3.32) and (4.13)]. For a massless field they are reduced to (3.34) and (4.14). The dependence of the FC on the magnetic flux becomes weaker with decreasing planar angle deficit. For points near the boundary, the contribution of the high-energy modes dominates in the expectation values and the leading term in the asymptotic expansion over the distance from the boundary coincides with that for the vacuum FC. In this region the effects of finite temperature, of planar angle deficit, and of magnetic flux are weak. As expected, at large distances from the boundary the FC is dominated by the Minkowskian term $\langle\bar{\psi}\psi\rangle_{\mathrm{M}}^{(0)}$, given by (3.29). For $Tr \gg 1$ the boundary-induced FC is exponentially suppressed. Similar behavior takes place for the topological part in the boundary-free FC. The behavior of the boundary-induced FC near the cone apex critically depends on the magnetic flux and on the planar angle deficit. It vanishes on the cone apex for $2|\alpha_0| < 1 - 1/q$ and diverges for $2|\alpha_0| > 1 - 1/q$. The divergence is related to the presence of the mode irregular at the cone apex. For a fixed distance from the boundary and at high temperatures the FC is dominated by the Minkowskian part.

We have also considered the FC for the boundary condition (4.17) that differs from the condition (2.6) by the sign of the term with the normal to the boundary. The corresponding formulas are obtained from those for the condition (2.6) by using the relations (4.21). In the special case of a massless field with zero chemical potential the FCs for the boundary conditions (2.6) and (4.17) differ by the sign only.

For a fermionic field realizing a irreducible representation of the Clifford algebra, the mass term breaks the P and T invariances. In order to construct P- and T-invariant models one can combine two fields corresponding to inequivalent representations. If both of the fields obey the boundary condition (2.6), the boundary-induced contribution in the total FC for this type of model is obtained from the results discussed in Secs. III and IV by using the relation (5.4) and it is an even function of the chemical potential and of the parameter α. Another possibility corresponds to the situation when the fields in different irreducible representations obey boundary conditions with different signs of the term involving the normal to the boundary. In this case the total FC is obtained with the help of the first relation in (5.4) where the separate terms are directly taken from the results in Secs. III and IV for the boundary condition (2.6). For a massless field the parts $\langle\bar{\psi}'_{(s)}\psi'_{(s)}\rangle^{(b)}$ do not depend on the parameter s and the total FC is zero. From the results presented in the present paper the FC can be obtained in graphitic cones with edges for the values of the opening angle $\phi_0 = 2\pi(1 - n_c/6)$ corresponding to even values of n_c (the number of the sectors with the angle $\pi/3$, excised from planar graphene).

ACKNOWLEDGMENTS

A. A. S. was supported by the CNPq Program APV, Process No. 453571/2018-2. E. R. B. M. was partially supported by CNPq through Project No. 313137/2014-5. Astghik Saharyan acknowledges additional support from the European Union's Horizon 2020 research and innovation program under the Marie Sklodowska-Curie Grant Agreement No. 765075 (LIMQUET).

APPENDIX A: ZERO CHEMICAL POTENTIAL

In this Appendix we consider the transformation of the mode-sum for the FC in the case of the zero chemical potential, $\mu = 0$. First we consider the exterior region, $r > a$. The boundary-induced contribution in the thermal part of the FC is given by the expression (3.9) with $\mu = 0$. Now the poles of the integrand are located on the imaginary axis:

$$E = E_n \equiv i\pi(2n+1)T, \qquad n = 0, \pm1, \pm2, \ldots, \tag{A1}$$

with $n = 0, \pm1, \pm2, \ldots$. For the values of $\gamma = \gamma_n$ corresponding to the poles (A1) in the upper half-plane one has

$$\gamma_n = iu_{0n}, \qquad n = 0, 1, 2, \ldots, \tag{A2}$$

with u_{0n} defined in (3.33), and for the poles in the lower half-plane we get $E_n^{(\lambda)} = E_{-n-1}^{(\lambda)*}$, $\gamma_n = \gamma_{-n-1}^*$,$n = \ldots, -2, -1$. As the next step, we rotate the integration contour in (3.9) by the angle $\pi/2$ for $l = 1$ and by the angle $-\pi/2$ for $l = 2$. The poles γ_n, $n = 0, \pm1, \pm2, \ldots$ are avoided by semicircles $C_\rho(\gamma_n)$ in the right half-plane with centers at $\gamma = \gamma_n$ and with small radius ρ. We get the following terms: the sum of the integrals over the straight segments of the positive and negative imaginary semiaxes between the poles γ_n and the sum of the integrals over the semicircles $C_\rho(\gamma_n)$. In the limit $\rho \to 0$ the sum of the integrals over the straight segments gives the principal values of the integrals over the positive and negative imaginary semiaxes (denoted here as p.v.). The integrals over the intervals $(0, im)$ and $(0, -im)$ cancel each other, whereas the integral over $(-im, -i\infty)$ is the complex conjugate of the integral over $(im, i\infty)$. For the sum of the integrals along the semicircles $C_\rho(\gamma_n)$, $n = 0, 1, 2, \ldots$, one gets

$$\sum_{n=0}^{\infty} \int_{C(\gamma_n)} d\gamma \frac{\bar{J}_{\beta_j}^{(\lambda)}(\gamma a)}{\bar{H}_{\beta_j}^{(1,\lambda)}(\gamma a)} [(E + \lambda sm) H_{\beta_j}^{(1)2}(\gamma r) - (E - \lambda sm) H_{\beta_j+\epsilon_j}^{(1)2}(\gamma r)] \frac{\gamma/E}{e^{\beta E} + 1}$$
$$= -2T \sum_{n=0}^{\infty} \frac{\bar{I}_{\beta_j}^{(\lambda)}(u_{0n}a)}{\bar{K}_{\beta_j}^{(\lambda)}(u_{0n}a)} [(i\pi(2n+1)T + \lambda sm) K_{\beta_j}^2(u_{0n}r) + (i\pi(2n+1)T - \lambda sm) K_{\beta_j+\epsilon_j}^2(u_{0n}r)], \tag{A3}$$

where the notations for the modified Bessel functions with the bar are defined in accordance of (3.14) with $\sqrt{(e^{\pi i/2}u_{0n}a)^2 + m_a^2} = i\pi(2n+1)Ta$. It can be seen that the sum of the integrals for $C_\rho(\gamma_n)$ with $n = \ldots, -2, -1$ is the complex conjugate of the right-hand side of (A3). Introducing the modified Bessel functions in the integral over $(im, i\infty)$ we get

$$\langle\bar{\psi}\psi\rangle_{T\lambda}^{(b)} = \lambda \frac{1}{\pi\phi_0} \sum_j \text{p.v.} \int_m^\infty dx \, \text{Im}\left\{ \frac{x}{e^{i\beta\sqrt{x^2-m^2}} + 1} \frac{\bar{I}_{\beta_j}^{(\lambda)}(xa)}{\bar{K}_{\beta_j}^{(\lambda)}(xa)} \left[\left(1 - \frac{\lambda ism}{\sqrt{x^2 - m^2}}\right) K_{\beta_j}^2(xr) + \left(1 + \frac{\lambda ism}{\sqrt{x^2 - m^2}}\right) K_{\beta_j+\epsilon_j}^2(xr) \right] \right.$$
$$\left. - \lambda \frac{T}{\phi_0} \sum_j \sum_{n=0}^{\infty} \text{Im}\left\{ \frac{\bar{I}_{\beta_j}^{(\lambda)}(u_{0n}a)}{\bar{K}_{\beta_j}^{(\lambda)}(u_{0n}a)} [(\pi(2n+1)T - \lambda ism) K_{\beta_j}^2(u_{0n}r) + (\pi(2n+1)T + \lambda ism) K_{\beta_j+\epsilon_j}^2(u_{0n}r)] \right\}. \tag{A4}$$

Now, by using the relations $\bar{I}^{(-)}_{\beta_j}(z) = \bar{I}^{(+)*}_{\beta_j}(z)$, $\bar{K}^{(-)}_{\beta_j}(z) = \bar{K}^{(+)*}_{\beta_j}(z)$, we can see that the contributions from the first term on the right-hand side of (A4) to the sum $\langle\bar{\psi}\psi\rangle^{(b)}_T = \sum_{\lambda=\pm}\langle\bar{\psi}\psi\rangle^{(b)}_{T\lambda}$ give $-\langle\bar{\psi}\psi\rangle^{(b)}_{\rm vac}$ and one finds

$$\langle\bar{\psi}\psi\rangle^{(b)}_T = -\frac{2T}{\phi_0}\sum_j\sum_{n=0}^{\infty}\mathrm{Im}\left\{\frac{\bar{I}_{\beta_j}(u_{0n}a)}{\bar{K}_{\beta_j}(u_{0n}a)}[(\pi(2n+1)T-ism)K^2_{\beta_j}(u_{0n}r)+(\pi(2n+1)T+ism)K^2_{\beta_j+\epsilon_j}(u_{0n}r)]\right\} - \langle\bar{\psi}\psi\rangle^{(b)}_{\rm vac}. \tag{A5}$$

For the total boundary-induced FC (3.25) the last term on the right of (A5) is canceled by the boundary-induced part in the vacuum FC, $\langle\bar{\psi}\psi\rangle^{(b)}_{\rm vac}$, and we get the representation (3.32) for the boundary-induced FC in the case of zero chemical potential. The corresponding formula is also obtained from (3.22) in the limit $\mu \to 0$.

Now let us consider the interior region, $r < a$. The thermal contributions to the FC coming from particles and antiparticles are given by (4.3) with $\mu = 0$. For the zero chemical potential the procedure we have used to obtain the summation formula (4.6) from the generalized Abel-Plana formula should be modified by taking into account that the function in the integrand has poles $z = \pm i\gamma_n = \pm iu_{0n}a$, $n = 0, 1, 2, \ldots$ on the imaginary axis, corresponding to the zeros of $e^{\beta\sqrt{z^2/a^2+m^2}} + 1$. In the part of the generalized Abel-Plana formula corresponding to the integral along the imaginary axis these poles are avoided by the semicircles $C_\rho(\gamma_n)$. In the limit $\rho \to 0$ we get

$$\begin{aligned}\sum_{l=1}^{\infty}T_{\beta_j}(\gamma^{(\lambda)}_{j,l})f(\gamma^{(\lambda)}_{j,l}) &= \int_0^\infty dx\, f(x) + \frac{\pi}{2}\mathop{\mathrm{Res}}_{z=0}\frac{\tilde{Y}^{(\lambda)}_{\beta_j}(z)}{\tilde{J}^{(\lambda)}_{\beta_j}(z)}f(z) \\ &\quad - 2\sum_{n=0}^{\infty}\mathrm{Re}\left[e^{-i\pi\beta_j}\frac{\tilde{K}^{(\lambda)}_{\beta_j}(u_{0n})}{\tilde{I}^{(\lambda)}_{\beta_j}(u_{0n})}\mathop{\mathrm{Res}}_{z=iu_{0n}}f(z)\right] \\ &\quad - \frac{2}{\pi}\mathrm{p.v.}\int_0^\infty dx\,\mathrm{Re}\left[e^{-i\pi\beta_j}f(xe^{\pi i/2})\frac{\tilde{K}^{(\lambda)}_{\beta_j}(x)}{\tilde{I}^{(\lambda)}_{\beta_j}(x)}\right].\end{aligned} \tag{A6}$$

Note that in applying this formula to the FC the term coming from the poles iu_{0n} is present for both $\lambda = +$ and $\lambda = -$, whereas in (4.6) the pole term is present only in case $\lambda\mu > 0$. Further transformations of the FC are similar to those for the exterior region. In the region $r < a$, the expressions for $\langle\bar{\psi}\psi\rangle^{(b)}_{T\lambda}$ and $\langle\bar{\psi}\psi\rangle^{(b)}_T$ are obtained from (A4) and (A5) by the replacements $I \rightleftarrows K$, $\bar{I} \to \tilde{I}$, and $\bar{K} \to \tilde{K}$. We see that the expression for $\langle\bar{\psi}\psi\rangle_b$ is also directly obtained from (4.10) in the limit $\mu \to 0$.

APPENDIX B: ZERO TEMPERATURE LIMIT

In this section we consider the zero temperature limit of the expressions for the FC obtained above. First of all for $|\mu| < m$ from (2.11) it follows that $\lim_{T\to 0}\langle\bar{\psi}\psi\rangle = \langle\bar{\psi}\psi\rangle_{\rm vac}$ and the FC coincides with that for the vacuum state. In the case $|\mu| > m$ and for the exterior region one gets

$$\begin{aligned}\lim_{T\to 0}\langle\bar{\psi}\psi\rangle &= \langle\bar{\psi}\psi\rangle_{\rm vac} + \lambda\frac{1}{2\phi_0}\sum_j\int_0^{\sqrt{\mu^2-m^2}}d\gamma\frac{\gamma}{E} \\ &\quad\times\frac{(E+\lambda sm)g^{(\lambda)2}_{\beta_j,\beta_j}(\gamma a,\gamma r)-(E-\lambda sm)g^{(\lambda)2}_{\beta_j,\beta_j+\epsilon_j}(\gamma a,\gamma r)}{\bar{J}^{(\lambda)2}_{\beta_j}(\gamma a)+\bar{Y}^{(\lambda)2}_{\beta_j}(\gamma a)},\end{aligned} \tag{B1}$$

where $\lambda = +$ for $\mu > 0$ and $\lambda = -$ for $\mu < 0$ ($\mu = \lambda|\mu|$). For the interior region

$$\langle\bar{\psi}\psi\rangle = \langle\bar{\psi}\psi\rangle_{\rm vac} + \lambda\frac{a^{-2}}{2\phi_0}\sum_j\sum_{l=1}^{l_m}T_{\beta_j}(\gamma^{(\lambda)}_{j,l})g(\gamma^{(\lambda)}_{j,l}), \tag{B2}$$

with the same λ as in (B1) and l_m defined by

$$\gamma^{(\lambda)}_{j,l_m} \le \sqrt{\mu^2-m^2} < \gamma^{(\lambda)}_{j,l_m+1}. \tag{B3}$$

The last terms in (B1) and (B2) come from particles for $\mu > 0$ and antiparticles for $\mu < 0$. They occupy the states with energies $E \le |\mu|$.

Now let us consider the limit $T \to 0$ for the boundary-induced contribution of the FC in the exterior region on the base of the formula (3.22). For small temperatures the dominant contribution to the sum over n in (3.22) comes from large values n and, to the leading order, we can replace the summation by the integration. The leading term does not depend on temperature and is presented as

$$\begin{aligned}\langle\bar{\psi}\psi\rangle^{(b)} &\approx -\frac{1}{\pi\phi_0}\sum_j\mathrm{Im}\left\{\int_{-i\mu}^{\infty-i\mu}dx\frac{\bar{I}_{\beta_j}(ua)}{\bar{K}_{\beta_j}(ua)}\right. \\ &\quad\left.\times[(x-ism)K^2_{\beta_j}(ur)+(x+ism)K^2_{\beta_j+\epsilon_j}(ur)]\right\},\end{aligned} \tag{B4}$$

where $u=(x^2+m^2)^{1/2}$. The integral on the right-hand side can be written as the sum of two integrals: $\int_{-i\mu}^{\infty-i\mu}dx=\int_0^\infty dx+\int_{-i\mu}^0 dx$. The part in the FC with the integral $\int_0^\infty dx$ coincides with the boundary-induced FC in the vacuum state. For $|\mu|<m$, introducing in the integral $\int_{-i\mu}^0 dx$ the integration variable $y=-ix$, we can see that the corresponding integral under the imaginary sign is real and, hence, the contribution of the integral $\int_{-i\mu}^0 dx$ to the FC is zero. Consequently, we get $\lim_{T\to 0}\langle\bar\psi\psi\rangle^{(b)}=\langle\bar\psi\psi\rangle^{(b)}_{\rm vac}$.

For $|\mu|>m$, we decompose the second integral as $\int_{-i\mu}^0 dx=\int_{-i\mu}^{-\lambda im}dx+\int_{-\lambda im}^0 dx$, where λ is defined by the relation $\mu=\lambda|\mu|$. The contribution of part with the integral $\int_{-\lambda im}^0 dx$ to the FC is zero by the same reason as that for the integral $\int_{-i\mu}^0 dx$ in the case $|\mu|<m$. In the integral $\int_{-i\mu}^{-\lambda im}dx$ we introduce y in accordance with $x=-\lambda iy$ and then pass to a new integration variable $z=\sqrt{y^2-m^2}$. Introducing the Bessel and Hankel functions instead of the modified Bessel functions, the limiting value of the boundary-induced FC is presented in the form

$$\lim_{T\to 0}\langle\bar\psi\psi\rangle^{(b)}=\langle\bar\psi\psi\rangle^{(b)}_{\rm vac}-\lambda\frac{1}{2\phi_0}\sum_j\mathrm{Re}\left\{\int_0^{\sqrt{\mu^2-m^2}}dz\,z\frac{\bar J^{(\lambda)}_{\beta_j}(za)}{\bar H^{(l,\lambda)}_{\beta_j}(za)}\left[\left(1+\frac{\lambda sm}{\sqrt{z^2+m^2}}\right)H^{(l)2}_{\beta_j}(zr)-\left(1-\frac{\lambda sm}{\sqrt{z^2+m^2}}\right)H^{(l)2}_{\beta_j+\epsilon_j}(zr)\right]\right\}, \tag{B5}$$

where $\mu=\lambda|\mu|$, $l=1$ for $\lambda=+$, $l=2$ for $\lambda=-$, and we use the notation (2.16). This coincides with the boundary-induced part obtained from (B1) by using the relation (3.7).

Now we consider the zero temperature limit in the interior region, based on the representation (4.10) for the boundary-induced part. To leading order, we replace the summation over n by integration with the result

$$\lim_{T\to 0}\langle\bar\psi\psi\rangle^{(b)}=-\frac{1}{\pi\phi_0}\sum_j\mathrm{Im}\left\{\int_{-i\mu}^{\infty-i\mu}dx\frac{\tilde K_{\beta_j}(ua)}{\tilde I_{\beta_j}(ua)}[(x-ism)I^2_{\beta_j}(ur)+(x+ism)I^2_{\beta_j+\epsilon_j}(ur)]\right\}, \tag{B6}$$

where $u=(x^2+m^2)^{1/2}$. Similar to the case of the exterior region, we split the integral as $\int_{-i\mu}^{\infty-i\mu}dx=\int_0^\infty dx+\int_{-i\mu}^0 dx$. The part in the FC corresponding to the integral over $[0,\infty)$ gives $\langle\bar\psi\psi\rangle^{(b)}_{\rm vac}$ [see (4.1)]. For $|\mu|<m$ and for the integral over $[-i\mu,0]$, in the arguments of the modified Bessel functions u is positive. Introducing a new integration variable $y=i\lambda x$, we see that the integral is real and does not contribute to (B6). Hence, for $|\mu|<m$, again we get $\lim_{T\to 0}\langle\bar\psi\psi\rangle^{(b)}=\langle\bar\psi\psi\rangle^{(b)}_{\rm vac}$. In the case $|\mu|>m$, the nonzero contribution comes from the part of the integral over $[-i\mu,-\lambda im]$. In addition we should take into account that the integrand in (B6) may have poles corresponding to $ua=-\lambda i\gamma^{(\lambda)}_{j,l}$, $l=1,2,\ldots,l_m$ [defined by (B3)] in that segment of the imaginary axis. Passing to a new integration variable $z=\lambda i(x^2+m^2)^{1/2}$, we avoid possible poles $z=\gamma^{(\lambda)}_{j,l}/a$ by small semicircles $C_\rho(\gamma^{(\lambda)}_{j,l}/a)$ in the right-half plane with a small radius ρ and with the center at $z=\gamma^{(\lambda)}_{j,l}/a$. In the limit $\rho\to 0$, the sum of the integrals over the straight segments between the poles gives the principal value of the integral and we get the following representation:

$$\lim_{T\to 0}\langle\bar\psi\psi\rangle^{(b)}=\langle\bar\psi\psi\rangle^{(b)}_{\rm vac}-\frac{1}{\pi\phi_0}\sum_j\mathrm{Im}\left\{\left[\mathrm{p.v.}\int_0^{\sqrt{\mu^2-m^2}}dz-\sum_{l=1}^{l_m}\int_{C_\rho(\gamma^{(\lambda)}_{j,l}/a)}dz\right]z\frac{\tilde K_{\beta_j}(ua)}{\tilde I_{\beta_j}(ua)}\right.$$
$$\left.\times\left[\left(1+\frac{\lambda sm}{\sqrt{z^2+m^2}}\right)I^2_{\beta_j}(ur)+\left(1-\frac{\lambda sm}{\sqrt{z^2+m^2}}\right)I^2_{\beta_j+\epsilon_j}(ur)\right]_{u=-\lambda iz}\right\}. \tag{B7}$$

By using the relations $\tilde J^{(\lambda)\prime}_{\beta_j}(w)=-2/[T^{(\lambda)}_{\beta_j}(w)J_{\beta_j}(w)]$ and $\tilde Y^{(\lambda)}_{\beta_j}(x)=2/[\pi J_{\beta_j}(x)]$, valid for $w=\gamma^{(\lambda)}_{j,l}$, it can be shown that the integral over $C_\rho(\gamma^{(\lambda)}_{j,l}/a)$ is equal to $\lambda i\pi T^{(\lambda)}_{\beta_j}(w)g(w)/(2a^2)$. Introducing in the integral over $[0,\sqrt{\mu^2-m^2}]$ the Bessel and Hankel functions, the integrand becomes $\tilde H^{(l,\lambda)}_{\beta_j}(za)g(za)/\tilde J^{(\lambda)}_{\beta_j}(za)$ with the real part $g(za)$. As a result, the zero-temperature limit is presented as

$$\lim_{T\to 0}\langle\bar\psi\psi\rangle^{(b)}=\langle\bar\psi\psi\rangle^{(b)}_{\rm vac}-\lambda\frac{1}{2\phi_0 a}\sum_j\int_0^{\sqrt{\mu^2-m^2}}dz\,g(za)+\lambda\frac{a^{-2}}{2\phi_0}\sum_j\sum_{l=1}^{l_m}T^{(\lambda)}_{\beta_j}(\gamma^{(\lambda)}_{j,l})g(\gamma^{(\lambda)}_{j,l}). \tag{B8}$$

From (4.4) it follows that $g(za)/a$ does not depend on a. By taking into account that for the boundary-free geometry one has

$$\lim_{T\to 0}\langle\bar{\psi}\psi\rangle^{(0)} = \langle\bar{\psi}\psi\rangle^{(0)}_{\rm vac} + \lambda\frac{1}{2\phi_0 a}\sum_j \int_0^{\sqrt{\mu^2-m^2}} dz\, g(za), \tag{B9}$$

we see that in the zero-temperature limit for the total FC the integral term in (B8) is canceled by the last term in (B9) and the formula (B2) is obtained. Hence, we have shown that both the representations for exterior and interior FCs give the same zero-temperature limit.

[1] N. Nagaosa, *Quantum Field Theory in Condensed Matter Physics and Quantum Field Theory in Strongly Correlated Electronic Systems* (Springer, Berlin, 1999).
[2] G. V. Dunne, *Topological Aspects of Low Dimensional Systems* (Springer, Berlin, 1999).
[3] E. Fradkin, *Field Theory of Condensed Matter Systems* (Cambridge University Press, Cambridge, England, 2013).
[4] E. C. Marino, *Quantum Field Theory Approach to Condensed Matter Physics* (Cambridge University Press, Cambridge, England, 2017).
[5] V. P. Gusynin, S. G. Sharapov, and J. P. Carbotte, Int. J. Mod. Phys. B **21**, 4611 (2007).
[6] A. H. C. Neto, F. Guinea, N. M. R. Peres, K. S. Novoselov, and A. K. Geim, Rev. Mod. Phys. **81**, 109 (2009).
[7] X.-L. Qi and S.-C. Zhang, Rev. Mod. Phys. **83**, 1057 (2011).
[8] S. Deser, R. Jackiw, and S. Templeton, Ann. Phys. (N.Y.) **140**, 372 (1982).
[9] A. J. Niemi and G. W. Semenoff, Phys. Rev. Lett. **51**, 2077 (1983).
[10] I. L. Buchbinder and E. N. Kirillova, Int. J. Mod. Phys. A **04**, 143 (1989); E. Elizalde, S. D. Odintsov, and Yu. I. Shil'nov, Mod. Phys. Lett. A **9**, 931 (1994); E. Elizalde, S. Leseduarte, and S. D. Odintsov, Phys. Rev. D **49**, 5551 (1994); Phys. Lett. B **347**, 33 (1995); D. K. Kim and G. Koh, Phys. Rev. D **51**, 4573 (1995); E. Elizalde and S. D. Odintsov, Phys. Rev. D **51**, 5990 (1995); E. Elizalde, S. Leseduarte, S. D. Odintsov, and Yu. I. Shil'nov, Phys. Rev. D **53**, 1917 (1996); T. Inagaki, T. Muta, and S. D. Odintsov, Prog. Theor. Phys. Suppl. **127**, 93 (1997); Yu. A. Sitenko, Phys. Rev. D **60**, 125017 (1999); Mod. Phys. Lett. A **14**, 701 (1999); A. Flachi, Phys. Rev. D **88**, 085011 (2013); E. V. Castro, A. Flachi, P. Ribeiro, and V. Vitagliano, Phys. Rev. Lett. **121**, 221601 (2018); A. Flachi and V. Vitagliano, Phys. Rev. D **99**, 125010 (2019).
[11] S. Bellucci, E. R. B. de Mello, and A. A. Saharian, Phys. Rev. D **83**, 085017 (2011).
[12] E. R. B. de Mello, V. Bezerra, A. A. Saharian, and V. M. Bardeghyan, Phys. Rev. D **82**, 085033 (2010).
[13] E. R. B. de Mello, F. Moraes, and A. A. Saharian, Phys. Rev. D **85**, 045016 (2012).
[14] S. Bellucci, E. R. B. de Mello, E. Bragança, and A. A. Saharian, Eur. Phys. J. C **76**, 350 (2016).
[15] A. Mohammadi, E. R. B. de Mello, and A. A. Saharian, J. Phys. A **48**, 185401 (2015).
[16] I. Brevik and T. Toverud, Classical Quantum Gravity **12**, 1229 (1995).
[17] E. R. B. de Mello, V. B. Bezerra, and A. A. Saharian, Phys. Lett. B **645**, 245 (2007).
[18] V. V. Nesterenko and I. G. Pirozhenko, Classical Quantum Gravity **28**, 175020 (2011).
[19] E. R. B. de Mello, V. B. Bezerra, A. A. Saharian, and A. S. Tarloyan, Phys. Rev. D **74**, 025017 (2006).
[20] E. R. B. de Mello, V. B. Bezerra, A. A. Saharian, and A. S. Tarloyan, Phys. Rev. D **78**, 105007 (2008).
[21] G. Fucci and K. Kirsten, J. High Energy Phys. 03 (2011) 016; J. Phys. A **44**, 295403 (2011).
[22] E. R. B. de Mello and A. A. Saharian, Classical Quantum Gravity **28**, 145008 (2011).
[23] E. R. B. de Mello, A. A. Saharian, and A. K. Grigoryan, J. Phys. A **45**, 374011 (2012).
[24] E. R. B. de Mello, A. A. Saharian, and S. V. Abajyan, Classical Quantum Gravity **30**, 015002 (2013).
[25] A. K. Grigoryan, A. R. Mkrtchyan, and A. A. Saharian, Int. J. Mod. Phys. D **26**, 1750064 (2017).
[26] E. R. B. de Mello, A. A. Saharian, and S. V. Abajyan, Phys. Rev. D **97**, 085023 (2018).
[27] E. R. B. de Mello and A. A. Saharian, Classical Quantum Gravity **29**, 035006 (2012); Eur. Phys. J. C **73**, 2532 (2013); S. Bellucci, E. R. B. de Mello, A. de Padua, and A. A. Saharian, Eur. Phys. J. C **74**, 2688 (2014).
[28] P. de Sousa Gerbert and R. Jackiw, Commun. Math. Phys. **124**, 229 (1989); Phys. Rev. D **40**, 1346 (1989); Yu. A. Sitenko, Ann. Phys. (N.Y.) **282**, 167 (2000).
[29] Yu. A. Sitenko and N. D. Vlasii, Nucl. Phys. **B787**, 241 (2007).
[30] M. F. Lin and D. S. Chuu, Phys. Rev. B **57**, 6731 (1998); S. Latil, S. Roche, and A. Rubio, Phys. Rev. B **67**, 165420 (2003).
[31] A. A. Saharian and E. R. Bezerra de Mello, J. Phys. A **37**, 3543 (2004).
[32] A. A. Saharian, Izvestiia Akademii nauk Armianskoi SSR Matematika **22**, 166 (1987) [Sov. J. Contemp. Math. Anal. **22**, 70 (1987)].
[33] A. A. Saharian, arXiv:0708.1187.
[34] M. V. Berry and R. J. Mondragon, Proc. R. Soc. A **412**, 53 (1987).
[35] P. Recher, B. Trauzettel, A. Rycerz, Ya. M. Blanter, C. W. J. Beenakker, and A. F. Morpurgo, Phys. Rev. B **76**, 235404 (2007).

[36] A. Krishnan, E. Dujardin, M. M. J. Treacy, J. Hugdahl, S. Lynum, and T. W. Ebbesen, Nature (London) **388**, 451 (1997); S. N. Naess, A. Elgsaeter, G. Helgesen, and K. D. Knudsen, Sci. Technol. Adv. Mater. **10**, 065002 (2009).

[37] P. E. Lammert and V. H. Crespi, Phys. Rev. Lett. **85**, 5190 (2000).

[38] J.-Ch. Charlier and G.-M. Rignanese, Phys. Rev. Lett. **86**, 5970 (2001).

[39] V. A. Osipov and E. A. Kochetov, JETP Lett. **73**, 562 (2001).

[40] P. E. Lammert and V. H. Crespi, Phys. Rev. B **69**, 035406 (2004).

[41] A. Cortijo and M. A. H. Vozmediano, Nucl. Phys. **B763**, 293 (2007).

[42] C. Furtado, F. Moraes, and A. M. M. Carvalho, Phys. Lett. A **372**, 5368 (2008).

[43] Yu. A. Sitenko and N. D. Vlasii, J. Phys. A **41**, 164034 (2008).